University of Alberta
Department of Civil Engineering

Structural Engineering Report No. 79

Fatigue Strength of Welded Steel Elements

by

M.P. Comeau

and

G.L. Kulak

October, 1979

FATIGUE STRENGTH OF WELDED STEEL ELEMENTS

by

M. P. COMEAU

and

G. L. KULAK

DEPARTMENT OF CIVIL ENGINEERING

THE UNIVERSITY OF ALBERTA

EDMONTON, ALBERTA

OCTOBER 1979

ABSTRACT

This investigation was conducted in two phases. In the first phase the fatigue behavior of fifteen steel beams with welded attachments was studied. In the second phase the fatigue behavior of four HSS trusses with welded connections was examined. Throughout the study the research findings were compared to the fatigue provisions of the Canadain Standards Association Standard S16.1-1974.

The beam tests were of two types, beams with lateral bracing attachments, and beams with plates intersecting the web. The study indicates that providing a 2:1 taper in the lateral bracing attachments does not improve fatigue life over providing a 90-degree transition. However, it was found that providing a circular transition significantly improves fatigue life. This is in agreement with the present code provisions. The study also indicates that beams with plates intersecting the web have essentially the same fatigue life as a beam with cover plates.

The study of HSS trusses with welded connections indicted that fatigue life for this type of detail is significantly less than that of a cover-plated beam.

ACKNOWLEDGEMENTS

This study was carried out in the Department of Civil Engineering at the University of Alberta. Fianancial assistance was provided by the National Research Council of Canada and by the Canadian Steel Industries Construction Council.

The authors also wishes to express their thanks to the technical staff of the Department of Civil Engineering for their assistance during the test program and to the Steel Company of Canada for providing the hollow structural shapes used in Phase II of this study.

Table of Contents

List of Figures

List of Tables

1. INTRODUCTION

1.1 General

Fatigue failure is a progressive failure which occurs as a consequence of repeated applications of stress and is initated by plastic movement within a localized region. Fatigue cracks can grow from micro to macro size as repetitive loading occurs.

In the early history of engineering, the fatigue problem was one which mainly concerned the mechanical engineer in the design of machine shafts, axles, and other mechanisms where stresses are applied repeatedly. More recently, fatigue cracking has become a concern for civil engineers. With the advent of new welding techniques, welds are now a primary fastener in most steel structures. Fatigue behavior must be considered as carefully as the evaluation of static strength when designing welded joints and members which will be subjected to repetitive loading.

Along with the widespread use of welds, present steel structures are less conservative than previous designs, due to a better understanding of member behavior. Coupled with this, live loads have either increased, as in highway bridges, or remained relatively constant, as in the case of overhead cranes and conveyor supports. Taking into account these two items it can be seen why fatigue is an important structural design consideration. The greater permissible member stresses result in an increased stress range, and live load stress range is a primary consideration in assessing fatigue behavior.

Fatigue cracks generally propagate through a material in a direction perpendicular to the applied stress. These cracks initiate at a micro-flaw within the structure of the material. These micro-flaws act as stress-raisers and increase the average local stresses to stresses at the tip of the flaw which are above the yield stress (1). Because of this, each time the nominal stress is applied, plastic deformation of the material at the flaw tip occurs and the crack may propagate through the material.

Micro-flaws are present in all engineering materials, but not all flaws will propagate into fatigue cracks. Only those flaws which are greater than the critical flaw size for a given stress intensity range will grow into fatigue cracks. In civil engineering structures, the type of structural detail greatly influences the initial flaw size. This is why type of detail is one of the governing factors in fatigue strength considerations for steel members.

1.2 Statement of Problem

Prior to about 1970, it was believed that the fatigue behavior of a structural member was adequately described by a consideration of the stress ratio and material yield stress (2). The influence of some details, such as as-rolled steel, groove or fillet welded joints, and bolted joints was also considered. Since then, work carried out by Fisher et al. (3,4) has shown that fatigue behavior can be mainly described by:

a. Stress range, that is, the algebraic difference between the maximum stress and the minimum stress at the detail.

b. Number of load applications.
c. Type of structural detail.

The present design codes of the Canadian Standards Association (CSA) (5,6,7) and the American Association of State Highway and Transportation Officials (AASHTO) (8) base their fatigue design requirements mainly on work carried out under the National Cooperative Highway Research Program (NCHRP) (3,4). In these standards a number of common structural details are grouped into design categories.

Not all structural details classified by the CSA and AASHTO Standards have been tested for fatigue performance; some have been assigned to their categories based on engineering judgement, and/or on theoretical analysis of stress concentration and crack growth (9). As a consequence, there exists a certain element of uncertainty in the classification of some details. This leads to the possibility that some of the predictions based on the present standards will be unconservative. In addition, in the particular case of welded hollow structural section (HSS) truss connections, none of these standards give any explicit information regarding evalulation for fatigue strength.

1.3 Objectives

The objectives of this study are:

a. To investigate the fatigue strength of beams with two specific types of fillet welded lateral bracing attachments.
b. To investigate the fatigue strength of beams with plates passing through, and fillet welded to, their webs.
c. To investigate the fatigue strength of welded trusses made up of square and rectangular HSS members.
d. To relate actual test data to results obtained using a fracture mechanics approach.
e. To recommend code revisions, if appropriate.

2. LITERATURE SURVEY

2.1 Previous Testing of Sections with Fillet Welded Attachments

Early investigations into the fatigue behavior of steel members with fillet welded flange or web attachments are relatively few. Some early tests were carried out by Gurney (10) wherein flat plates with attachments fillet welded to their edges were repetitively loaded in tension. Attachments of two lengths, eight inches and four inches were tested. It was found that the member with the shorter attachment had approximately a 20% longer fatigue life.

Gurney (2) states that discontinuous longitudinal welds result in a lower fatigue life than longitudinal welds which extend for the entire length of the member. This is due to the more severe stress concentrations in the case of the intermittent weld.

Tests carried out in Sweden and Germany, reported by Gurney (2), have shown that local machining of the weld ends of fillet welded attachments can give an increase in fatigue life of from 37% to 80%. This local machining consists of grinding down the weld end, thus removing the weld toe, and decreasing the stress concentration at the weld termination.

The first comprehensive testing of actual beams with welded attachments was carried out in the National Cooperative Highway Research Program (NCHRP) series of tests (4). In this study, 59 beams with fillet-welded flange attachments were tested. The attachment lengths ranged from 1/4 inch to eight inches. The fatigue life was found to decrease as the attachment length increased. The slopes of the mean regression lines for each attachment length were approximately equal, and in good agreement with the slopes for cover-plated and plain welded beams.

The CSA (5,6,7) and AASHTO (8) Standards base their recommendations on the results of the NCHRP tests (4). Attachments are classified as Category C, D, or E, depending on length. Welds less than two inches are Category C; welds between two inches and twelve times the plate thickness, but less than four inches are Category D; and welds greater than four inches long or twelve times the plate thickness are Category E. Bardell and Kulak (11) have tested a number of fillet welded attachments and their results agree closely with the NCHRP findings. In these tests, the attachments were welded to the web, whereas in the NCHRP tests attachments were welded to the flange. At the time they were drawn up, the AASHTO and CSA fatigue categories for fillet welded attachments were based on tests with attachments welded to the beam flanges.

The CSA and AASHTO standards also allow increased stress ranges for attachments with semi-circular transitions and ground weld ends. Transitions of between zero and two inch radius are Category E, between two inch and six inch are Category D, between six inches and 24 inches are Category C, and greater than 24 inches are Category B. These categories are not based on actual tests, but on analytical studies of the stress concentration conditions at the detail (9).

2.2 Previous Testing of Welded HSS Truss Connections

Knowledge of the fatigue behavior of welded HSS truss connections first became available in the mid-1960's. It was approximately at this time that design rules were developed for HSS connections under static loads. Since then, many joints have been tested in fatigue loading; however, entire trusses have generally not been tested for fatigue performance.

Early testing was carried out by Babiker (12) in England. Babiker tested N-type truss joints of the type shown in Fig. 2.1 with a square chord member and round web members. A compressive prestress was applied to the chord member prior to applying the pulsating load to the assembly. The pulsating load was applied to the vertical web member only and the diagonal web member held rigid. In this manner a pulsating load was induced into the diagonal web member and half of the chord member.

Babiker concluded that joints with 100% overlap of the web members gave the best fatigue performance. Gap joints had the worst fatigue life, and joints with 50% overlap fell between gap joints and 100% overlap (see Fig. 2.1 for definition of gap and overlap). He attributed the lower fatigue life for 50% overlap to intersection of the weld beads at the joint.

Tests carried out by Eastwood et al. (13) on 12 large joint specimens and 36 small joint specimens led to essentially the same conclusions as those presented by Babiker. The method of testing and type of joint were similar. In addition, Eastwood concluded that the stiffness of the chord member wall influenced fatigue performance. This was considered not as significant as the amount of overlap in the joint, however.

In a series of further tests, Eastwood, Wood, and Opie (14) showed that using rectangular hollow sections as web members (and also as chord members) improved fatigue life as compared to using circular web members. They also concluded that using a stiffener plate on the chord face to reinforce a gap joint does not signicantly improve the fatigue life of the joint as compared to overlapping of the web members. The above conclusions are further emphasized by Eastwood and Wood (15) in a research summary where some guidance is given as to how to design joints for fatigue loading.

Bouwkamp and Stephen (16,17) have investigated a number of tubular joints under alternating loads. In general, they have found that joints with thick-walled chord members perform better than those with thin-walled chord members. They also recommend that joints with intersecting welds should not be used. However, the investigations carried out by Bouwkamp and Stephen deal specifically with typical joints found in offshore structures. Their results were useful for comparison, but do not relate directly to the type of joints considered in the present study.

The use of gusset plates between web and chord members has also been investigated (17). No definite conclusion was drawn as to the effect of the gusset, but it was noted that scalloping the gusset improved life, compared to having a straight or tapered gusset.

Some full-scale trusses have been tested in Japan (18). The trusses tested had a 13 m (42.6 ft.) span and were 3.5 m (11.5 ft.) high (see Fig. 2.2). The members were box sections built up from individual plates. The web members were bolted to gusset plates welded on both sides of the chord member. Small joint specimens with the same detail as the full-scale specimens were also tested. The fatigue lives obtained in the full-scale tests were approximately 30% lower than those obtained from the small joint specimens. It was concluded that the lower fatigue strength in the full-scale specimens was due to the effect of residual stresses in the welds. This is the only test of an actual truss using rectangular section members that has been reported to date.

The Steel Company of Canada, Limited, (STELCO) has issued a design handbook (19) as an aid in proportioning welded connections between hollow structural sections (HSS). Some guidance for fatigue loading is given and this is based mainly on the work of Babiker (12) and Eastwood and Wood (15). The guidelines in the handbook are based on the stress ratio approach to fatigue performance, rather than the stress range concept.

2.3 Development of Present Code Requirements

The present fatigue design requirements of CSA (5,6,7) and AASHTO (8) are typical of those used in North America at the present time. They are based on the NCHRP series of tests (3,4,9,20) and reflect the conclusions that the stress range, number of cycles, and type of detail are the primary considerations for fatigue design. The three CSA Standards (S6,S16.1,W59) and the AASHTO Standard all have similar requirements for fatigue design. Based on this, reference will only be made to one standard, CSA S16.1, throughout the remainder of this report.

The NCHRP test series comprised 531 beams with a variety of details. From the results it was determined that a cover-plated beam gave the lowest fatigue life of all details tested, while a plain rolled section provided an upper limit to fatigue life. All other details tested fell between these two boundaries. Based on this, five fatigue categories were defined in CSA S16.1. Category A is an upper boundary, representing a plain rolled section. Category E describes the least fatigue life, and includes cover-plated beams. Between these, in order of diminishing fatigue life, are: plain welded beams, transverse stiffeners, groove welded splices, and longitudinal attachments. In the present design standard some details were assigned to categories based on their performance in the NCHRP tests, while other details were categorized according to engineering judgement and/or a theoretical analysis of stress concentration and crack growth.

The log-log plots of the fatigue categories are parallel and have a slope of -3. Each category is based on the mathematical model; Log N = A - B Log S_r where:

N = number of cycles

S_r = the stress range

A, B = constants for a particular design category.

The categories were chosen on the basis of the 95% confidence limits for 95% survival of a regression line analysis of the test data of a typical detail in each particular

category.

Subsequent to the NCHRP study, two additional fatigue categories have been created. The first, Category F, governs the fatigue strength of cover plated beams with a flange thickness greater than 3/4 inch. This category predicts fatigue lives which are lower than Category E. The second, Category W, governs allowable shear stress range on the throat of fillet welds. This category is not parallel to the other six. Above S_r = 10 ksi. it is below Category E and below S_r = 1 Category E.

The beam details being investigated in this study would be classified as follows by the CSA S16.1 Standard. Tapered transition lateral bracing attachments would be Category E, based on the fillet weld length. Circular transition lateral bracing attachments would be Category D, based on the four inch radius. Beams with members intersecting the webs are not explicitly mentioned in the Standard, but they could be classified as Category E, based on the length of fillet weld.

The present code does not give any explicit requirements for allowable stress ranges in welded HSS truss connections. However, based on the available design recommendations (19), and on previous testing of isolated HSS joints (12,13,14,15), fatigue strengths predicted by Category E or Category F would be expected for this type of detail.

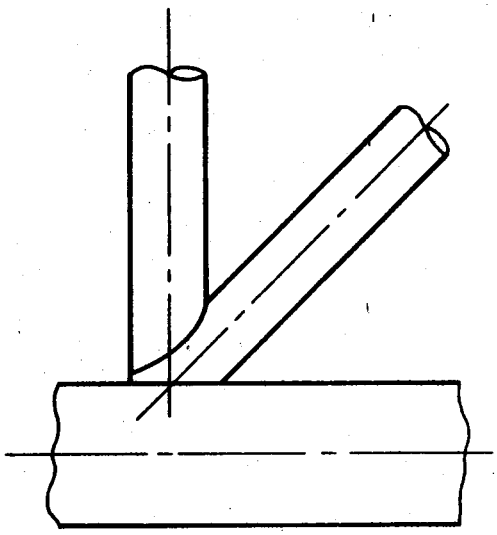

a. 100% Overlap

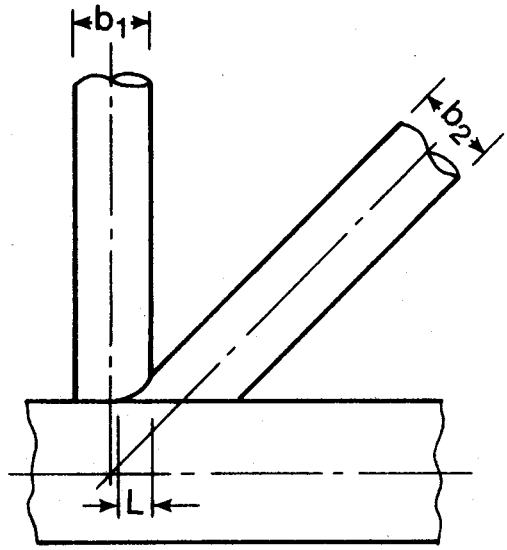

b. Partially Intersecting

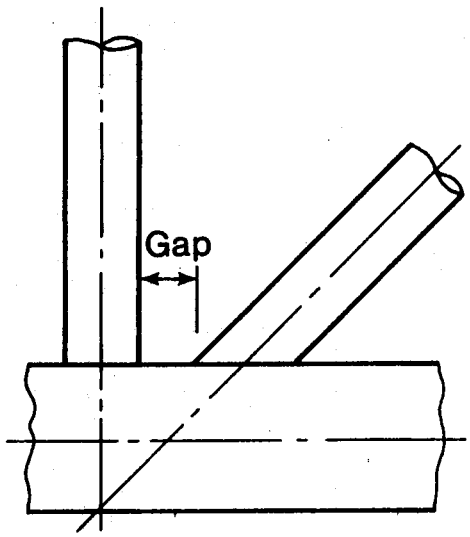

c. Gap Joint

$$\text{Overlap} = \frac{L}{\left(\frac{b_1 + b_2}{2}\right)}$$

Figure 2.1 Tubular Connection Details (Ref 12)

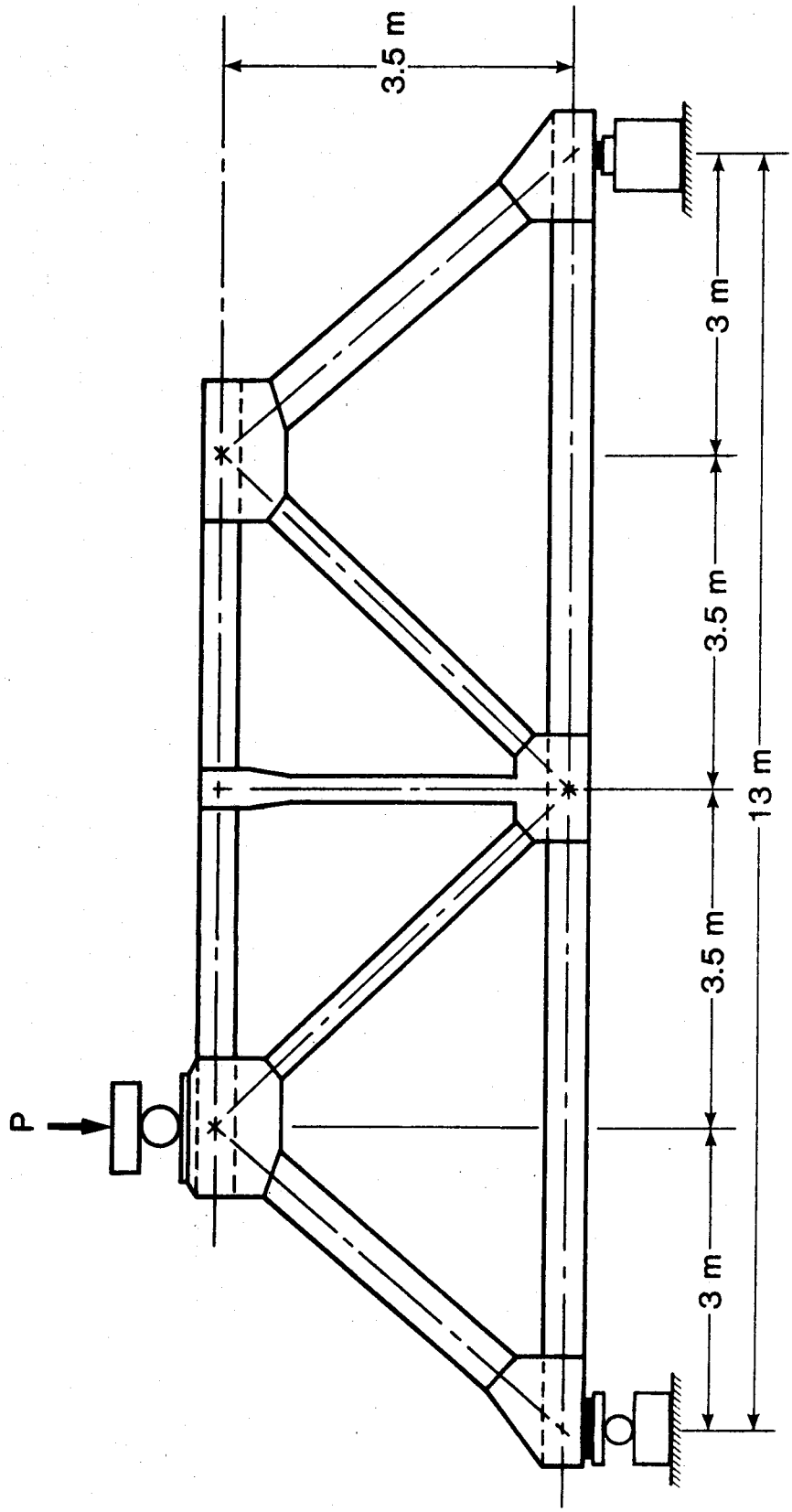

Figure 2.2 Truss Test Layout (Ref 18)

3. PHASE I - BEAMS WITH WELDED DETAILS

3.1 Experimental Program

3.1.1 Scope

Nine tests were used to investigate the fatigue strength of beams with two specific types of fillet welded lateral bracing attachments. Of these, three had a tapered transition horizontal gusset as shown in Figs. 3.1 and 3.3 (specimens 1T, 2T, 1TG), and six had a horizontal gusset with a circular transition as shown in Figs. 3.2 and 3.4 (Specimens 1RG to 6RG).

The three beams with tapered gussets were tested to see if provision of this type of transition would improve fatigue life as compared to the rectangular gussests tested by Bardell and Kulak (11). In one of the three beams (1TG), the weld toes at the ends of the attachment were ground out to see what effect this would have on the fatigue life. Fillet welded attachments with a tapered transition are not defined as a typical detail in CSA Standard S16.1.

The six beams with circular transition gusset plates were tested to investigate the validity of the CSA Standard's classification of this type of detail. The development of this detail in the Standard has primarily been based on a theoretical analysis of stress concentration and crack growth (9).

In addition, as part of Phase I, six beams were tested in which plates intersected and passed through the web of the test beam as shown in Figs. 3.5 and 3.7 (specimens 1W to 6W). The purpose of these tests was to simulate the conditions created when an intersecting member must pass through, and/or be welded to, a beam web at right angles. This may occur particularly in large plate girder or box girder structures, and also in some floor beam flange to girder web connections. Three of the beams investigated had an intersecting plate to web thickness ratio of 2.51 (specimens 1W, 2W and 3W) and three had an intersecting plate to web thickness ratio of 3.26 (specimens 4W, 5W, and 6W). In all six cases the thickness of the intersecting plate was 3/4 inch.

3.1.2 Beams With Lateral Bracing Attachments

3.1.2.1 Specimen Description

The nine beams tested in this series were all W16x36 hot-rolled sections. The grade of steel specified was CSA G40.21 44W (21) for the beams, the vertical stiffeners, and the horizontal gussets. All beams were 10 ft.-6 in. long.

Welding of vertical stiffeners and horizontal gussets was carried out at the University of Alberta, Structural Engineering Laboratory, by a welder certified by the Canadian Welding Bureau. Welds were done manually by the shielded-metal arc process using AWS E7024 electrodes. All welds were 1/4 in. fillets, and were inspected visually prior to testing of the members.

The beams with tapered horizontal gussets (T series) had details as shown in Figs.

3.1 and 3.3. The vertical stiffeners were 3/8 in. thick plate, 3-1/4 in. wide and 13-1/2 in. long. Stiffeners were fillet welded to the beam flange and web, and a 1 in. by 1 in. cope was provided at the top of each stiffener so that web and flange welds would not meet. The horizontal gussets were 5/16 in. thick plate, 4-3/4 in. wide and 29 in. long. As shown in Fig. 3.3, a 2:1 transition was provided at each end of the gusset. A 1/2 in. wide slot was saw-cut into each gusset so that it would fit over the vertical stiffener. The gusset was fillet welded to the beam web and to the vertical stiffener. Two 1 in. by 1 in. copes were provided so that no fillet welds would meet at the detail. All edges of the vertical stiffener and horizontal gusset were saw-cut edges.

On two beams, 1T and 2T, the fillet welds at the end of the horizontal gusset were left as-welded. On specimen 1TG the welds were ground down at the ends of the gusset, providing a smooth transition between gusset and beam web. Grinding was done manually, using a small electric grinder, and was carried out parallel to the length of the beam.

One stiffener - gusset detail was provided at the centerline of each beam tested. The gusset plates were attached at a distance of 2-7/16 in. from the extreme fiber of the beam in all three cases.

The stiffener - gusset detail for the six beams with circular transition horizontal gussets (RG series) is shown in Figs. 3.2 and 3.4. All six beams had vertical stiffeners identical to those of the three beams with tapered gussets. The horizontal gussets were made from 5/16 in. plate, 4-3/4 in. wide by 18 in. long. All had a 4 in. radius at each end. The fillet weld toe at the end of the circular transition was ground smooth. Grinding of the weld toe was done manually and was done in a direction parallel to the length of the beam. These gussets were saw-cut and coped in the same way as the tapered horizontal gussets. This detail is classified as Category D in the CSA Standard, but was not a detail tested in the NCHRP program.

One stiffener - circular transition gusset detail was provided at the centerline of each beam. The gusset plates were attached 2-7/16 in. from the extreme fiber of the beam in all six cases.

3.1.2.2 Test Set-Up

All specimens in this series (tapered transition and circular transition) were tested on a 10 ft. span. The load was applied symmetrically at two points using a spreader beam on a 3 ft.-6 in. span. All details tested were contained within the constant moment region created by this loading arrangement.

The reactions and load points were all simply supported by steel rockers. During the test, lateral support for the system was provided by bracing the spreader beam.

An Amsler testing system was used to apply the fatigue loading. The system uses a variable-stroke hydraulic pump (pulsator) to load a hydraulic jack. The jack has a maximum load capacity of 110 kips. The system has two fixed operating speeds, 250 and 500 cycles-per-minute. A speed of 500 cpm was used for the entire test series.

Since the dynamic response of the system is unknown, it is necessary to relate the static and dynamic loads. To do this, an oscilloscope was used in conjunction with strain gauges mounted on the test beam to calibrate the maximum and minimum load dials on the Amsler unit. The beam was first loaded to the desired minimum stress and the corresponding voltage output marked on the oscilloscope face. The process was then repeated for the maximum stress. The beam was then loaded at 500 cpm and the maximum and minimum dynamic loads adjusted until the limits corresponded to the marks on the oscilloscope. The values on the maximum and minimum load dials on the Amsler unit were then used as references for the remainder of the testing time.

3.1.2.3 Test Procedure

All nine beams with lateral bracing attachments were tested in a similar manner. The minimum extreme fiber stress was 4 ksi, providing a minimum stress of 2.78 ksi at the level of the detail. The stress range at the detail for the nine beams varied between 10 and 19 ksi.

The criterion used to determine failure of a beam was an increase in deflection of 0.02 in. A micro-switch placed at mid-span interrupted testing when the 0.02 in. increase occurred. In this manner, tests could be run continuously and without supervision until failure. The NCHRP test series (3,4) also used this criterion to define failure. At this point in the tests, crack propagation was rapid and 35% to 75% of the flange area remained uncracked.

Measurements of deflection and strain distribution in the gusset were carried out under static load, before beginning fatigue loading of the specimen.

When a crack at only one end of the gusset resulted in a failure, it was repaired by clamping extra plates on the flange. Using this method testing could be continued in an attempt to obtain a failure at the other end of the gusset. These repairs were successful in the majority of cases, enabling two test points to be obtained from most beams.

After testing, the portions containing fatigue cracks were flame cut out of the beam. Cracks were then saw-cut open and the fracture surface examined.

Stress ranges for beams 1T and 2T were chosen so that the results could be compared to the results obtained by Bardell and Kulak (11) for rectangular gusset plates. The stress range for specimen 1TG was chosen so that the test results could be compared directly to those of specimen 1T. Stress ranges for the RG series were chosen to provide a wide range on the present CSA Category D design curve, while also keeping above the proposed run-out stress range of 7 ksi.

3.1.3 Beams With Plates Intersecting the Webs

3.1.3.1 Specimen Description

Six beams were tested in this series (W series). Specimens 1W, 2W and 3W used W16x36 hot-rolled sections, while specimens 4W, 5W and 6W used W14x22 hot-rolled sections. All steel for the beams was CSA G40.21 44W (21), and all beams were 10 ft.-6 in. long. The plates welded to the beam webs were of ASTM A36 steel.

The detail investigated is shown in Figs. 3.5 and 3.7. All plates used were 3/4 in. thick and 7 in. wide. Each beam contained two different plate details. In detail A, one 12 in. long plate passed through a flame cut opening in the beam web. Detail B had two plates each 6 in. long welded to each side of the web. By using these configurations, a comparison could be made between the effect of passing the plate through the web and an interruption of the plate at the web. For both details 1/4 inch fillet welds were used. The plates were welded all around, on both sides of the beam web.

Plates were welded to the beam webs at the University of Alberta Structural Engineering Laboratory, by a welder certified by the Canadian Welding Bureau. Welds were done manually by the shielded-metal arc process, using AWS E7024 electrodes. All welds were inspected visually prior to testing.

Holes for the plate passing through the web allowed 1/8 in. extra in each direction for clearance. Any slag from the cutting process was removed by grinding prior to welding. The plates for all specimens were located such that a clear distance of 2 in. between the plate and the beam flange was provided.

The variables for this test series were stress range, type of detail (piercing the beam web, or interrupting the plate at the web), and plate to web thickness ratio.

3.1.3.2 Test Set-Up

All beams were tested on a 10 ft. span, with two point loading applied by a spreader beam on a 3 ft.-6 in. span. The test beam and spreader beam were all simply supported on steel rockers. With this test configuration, both web plate details were located completely within the constant moment region. During the test, lateral support was provided to the spreader beam.

The Amsler fatigue loading unit was calibrated for each test in the same manner as described for beams with lateral bracing attachments. The loading rate used was 500 cpm for all six beams.

3.1.3.3 Test Procedure

All six beams in the W series were tested in the same manner. The minimum extreme fiber stress was 4 ksi for all beams. This provided a minimum stress of 2.78 ksi at the level of the detail for beams 1W, 2W and 3W. The minimum stress at the detail was 2.64 ksi for beams 4W, 5W and 6W.

The criterion used to determine failure was a 0.02 in. increase in mid-span deflection. A micro-switch interrupted testing when this deflection increase was reached.

Beams in this series were also repaired by clamping plates on the flange. In this way as many failure points as possible were obtained per beam.

Before the fatigue testing was begun, beams were loaded statically to obtain strain distribution and deflection readings.

After completion of fatigue testing, damaged areas were flame cut from the beam. The fatigue cracks were then saw-cut open and the failure surfaces examined.

3.2 Test Results

3.2.1 Beams With Lateral Bracing Attachments

3.2.1.1 Crack Initiation and Growth

The crack initiation and growth patterns for specimens 1T and 2T were quite similar. Cracks initiated in the fillet weld at the end of the horizontal gusset with one crack appearing at each end of the gusset for each specimen. The cracks grew vertically upward and downward from the initiation site in the beam web.

At three crack locations the crack initiated at a slag inclusion and/or gas pocket in the weld, and not at the toe of the weld. One crack in specimen 2T grew from a flaw (undercut and/or slag inclusion) at the toe of the fillet weld.

The weld toes at the ends of the horizontal gusset were ground smooth on specimen 1TG. The purpose of this was to see whether improving the notch condition at the weld toe would increase the fatigue life. The two fatigue cracks which were observed in this beam initiated in the weld at the ends of the horizontal gusset as shown in Fig. 3.6. These cracks grew from internal slag inclusions and/or gas pockets. Neither of the two cracks observed formed where the weld toe had been present prior to grinding.

In the RG test series, cracks initiated at flaws in the weld at the end of the horizontal gusset. In all eight cracks observed, the cracks originated at slag inclusions and/or gas pockets in the weld. No cracks initiated at the location where the actual weld toe had been present prior to grinding. All cracks grew vertically upward and downward simultaneously from the initiation site. This is shown in Fig. 3.8.

Cracks in the RG test series were generally observed sooner in the fatigue life of the beam than cracks in specimens 1T and 2T. Also, cracks in the RG series seemed to propagate more slowly than those in specimens 1T and 2T. Often, a jog in the crack was observed, as shown in Fig. 3.8. These jogs indicated locations where two cracks had begun propagating independently from separate flaws. After merging, the two cracks continued to grow as one. The surface of this type of crack has a stepped appearance, as shown in Fig. 3.9.

In beam 5RG, failure occurred at the weld toe of the vertical stiffener and not at the end of the horizontal gusset. This failure occurred at 1,776,000 cycles, which is well beyond the predicted fatigue life for the type of flaw which would be expected in the weld at the end of the horizontal gusset. At the stress range applied to this specimen (15 ksi), it could be expected that the vertical stiffener weld would cause a failure at this number of cycles. Apparently the flaws that might have been present at the ends of the horizontal gusset were below critical size in this particular specimen, and the failure was controlled by the conditions at the vertical stiffener detail.

In the T and RG test series, cracks generally went through three phases as they

propagated to failure. The first phase involves growth from micro to macro size. In this phase, the crack grows as a semi-ellipse radiating outward from the initial flaw. The crack maintains this semi-elliptical shape for as long as it takes to grow through the beam web, provided it does not intersect with cracks growing simultaneously from other flaws. Between 60% and 85% of the fatigue life of the beam is consumed in the propagation of the crack through the web.

Once the crack has grown through the web, a second phase of the growth cycle begins. In this phase, the crack grows as a two-ended crack and continues to grow until the flange to web junction is reached and propagation through the flange occurs. Once the crack has grown through the flange, a third phase begins, in which the crack grows as a three-ended crack until the failure criterion is reached.

With the exception of specimen 5RG, previously described, all of the cracks causing failure in the T and RG series occurred at the horizontal gusset end welds. No cracks were observed at any other locations in the beam web or flanges, vertical stiffener, or horizontal gusset.

3.2.1.2 Effect of Stress Range

The stress range had a very significant effect on the fatigue life of each beam tested. In all tests the minimum extreme fiber stress was kept constant and only the stress range was varied. As expected, the fatigue life of a beam decreased as the stress range was increased.

The test results for specimens 1T and 2T are given in Table 3.1 and are plotted in Fig. 3.10. Each data point on the graph represents a fatigue crack at the detail. Some of the data points were obtained by repairing a fatigue crack at one end of the detail and continuing testing in order to obtain another data point from that beam. Two data points obtained from a pilot test carried out by Bardell and Kulak (11) on an identical detail have been plotted on the graph as well and are also included in the table.

A regression line analysis was carried out on the six data points using the linear model $\text{Log } N = A + B \text{ Log } S_r$. This line is plotted in Fig. 3.10. The equation $\text{Log } N = 9.292 - 3.095 \text{ Log } S_r$, which is the equation obtained by Fisher et al. (3) for the fatigue life of a cover plated beam, in Fig. 3.10 for purposes of comparison. The two data points obtained from specimen 1TG are also shown in Fig. 3.10, but these two points were not included in the regression line analysis.

The test results for lateral bracing attachments with a circular transition are presented in Table 3.2 and plotted in Fig. 3.11. Each data point represents a failure at one end of the horizontal gusset. Some of the data points were obtained by repairing a crack at one end of the horizontal gusset and continuing testing in order to obtain a failure at the other end. In specimens 1RG and 4RG it was only possible to obtain one data point for each beam, although testing was continued up to 2,240,500 and 8,086,500 cycles, respectively.

A regression line analysis using the linear model $\text{Log } N = A + B \text{ Log } S_r$ was

carried out on the eight data points and is shown in Fig. 3.11. The equation for the fatigue life of a cover plated beam, obtained by Fisher, is also plotted in the figure. Specimen 5RG, which failed at the vertical stiffener weld at 1,776,000 cycles has not been included in the analysis.

3.2.1.3 Effect of Transition in Lateral Bracing Attachment

A comparison of Fig. 3.10 with Fig. 3.11 shows that beams in which the lateral bracing attachment had a circular transition have a greater fatigue life than those beams in which a tapered transition is used. This comparison may be further extended to include beams tested by Bardell and Kulak (11) in which a similar lateral bracing attachment was used. In this case, the transition was a detail using a 90-degree change in direction, and the equation obtained from the test data is also shown in Fig. 3.10.

Comparing the three types of transition leads to the conclusion that using a 2:1 (26.6-degree) tapered transition does not give a notably better fatigue life than using the abrupt, 90-degree transition. Thus, the extra material and fabrication costs involved in the case of a tapered transition are not justified. If an increase in fatigue life is desired a circular transition with the weld end ground smooth must be used.

One specimen (1TG) was tested which had both a tapered transition and the weld end ground smooth. The test result has been plotted in Fig. 3.10. The fatigue life of the detail was not significantly improved by grinding, and no further details of this type were tested.

3.2.1.4 Stress Distribution in Attachments

It has been observed that the amount of load carried by attachments welded to a beam flange varies according to the length of the attachment. Fisher et al. (4), have shown that an attachment plate will develop its full capacity if it is three to four times as long as it is wide.

As a part of the study presented in this report, strain readings were taken at various locations on the lateral bracing attachments. All strains were measured parallel to the longitudinal direction of the beam. Gauges were positioned on the lateral bracing attachments as shown in Figs. 3.12 and 3.13. These measurements were taken on specimens 1T, 2T, 1TG, 1RG, 2RG and 3RG. The resulting stress distributions are shown in Figs. 3.14 and 3.15. The distance shown on the graph is the perpendicular distance from the beam web face.

The stress distributions measured for specimens 1T, 2T and 1TG are given in Fig. 3.14. All the readings on this figure were taken with an extreme fiber stress in the beam of about 32 ksi. Examining the readings taken 1-1/2 in. away from the line of the vertical stiffener, it can be seen that a straight line could be drawn through the data given for distances between 1-1/2 in. and 3-3/4 in. from the beam web. However, the data given for 3/4 in. from the beam web would fall significantly below this line. The existence of the cope in the horizontal gusset may possibly influence the data gathered at the 3/4 in. location.

The plot of data in Fig. 3.14 also gives the stress distribution in the horizontal

gusset 5 in. away from the line of the vertical stiffener. A straight line could be drawn through these data points and the non-linearity observed for data gathered at 3/4 in. from the beam web, is no longer present. In this case, it is likely that the readings were taken a sufficient distance from the cope that the cope did not affect the readings.

The stress distributions measured in specimens 1RG, 2RG and 3RG are given in Fig. 3.15. All these readings were taken at an extreme fiber stress in the beam of about 23 ksi. Again, the data gathered at 3/8 in. and 3/4 in. from the beam web would fall below a straight line drawn through the stresses measured at 2-1/4, 3-3/4 and 4-1/2 in. These readings were all taken 1-1/2 in. away from the line of the vertical stiffener. Here also, the presence of the cope could have an influence on these readings.

Strain readings at 3-3/4 in. and 4-1/2 in. away from the beam we 1RG, 2RG, and 3RG show that this region of the horizontal gusset is in compression. Also, the compressive force is increasing towards the edge of the horizontal gusset. These readings seem to indicate that the horizontal gusset is experiencing some type of bending phenomenon due to the strains induced in it by the beam web.

3.2.1.5 Comparison With Previous Studies

Fisher et al. (4) have tested a number of beams with attachments fillet welded to their flanges. The results of their testing program have formed a major part of the basis for classifying beams with fillet welded attachments as fatigue Category C, D, or E in the CSA design specification.

It has been found that as attachment length increases, the fatigue life of the detail decreases. Thus, the CSA specification has classified fillet welded attachments less than 2 in. long as Category C, fillet welded attachments with length between 2 in. and 12 times the plate thickness but less than 4 in. as Category D, and fillet welded attachments with length greater than 12 times the plate thickness or 4 in. as Category E.

Category E is based primarily on tests of cover-plated beams and they are a typical detail in this fatigue category. The tapered lateral bracing attachments have a fillet weld length of 13-1/4 in. and thus would be classified as Category E. The data points for these tests all fell above the 95% confidence line for 95% survival obtained from the tests of cover-plated beams as shown in Fig. 3.10. It is this line which is used as the basis for Category E in the CSA design specification.

Based on the data presented herein, it seems reasonable to classify tapered lateral bracing attachments as fatigue Category E. Tapering in itself does not improve the fatigue life of the detail, and the stress concentration condition at the weld toe seems to govern the fatigue life of the detail.

Lateral bracing attachments with circular transitions were not included in the testing programs carried out by Fisher et al. (3,4). However, this type of detail has been included in CSA Standard S16.1 based on an analytical study of the stress concentration conditions present at the weld ends.

The CSA design specification classifies circular transitions as follows: transitions with a radius greater than 24 in. are Category B; transitions with a radius less than 24 in. but not less than 6 in. are Category C; transitions with a radius less than 6 in. but not less than 2 in. are Category D; and transitions between zero and 2 in. are Category E. In addition, all circular transitions must have the weld end ground smooth. The lateral bracing attachment investigated in the present study is therefore classified as Category D by the CSA specification. The basis for Category D is the 95% confidence line for 95% survival obtained from tests carried out by Fisher (4) on beams with 4 in. long rectangular attachments welded to their flanges. All data points in the present test series fall on or above this line. Also, the regression line obtained from the data in the RG test series ($\text{Log } N = 8.956 - 2.554 \text{ Log } S_r$) plots within the 95% confidence interval obtained by Fisher for beams with 4 in. rectangular attachments. This is shown in Fig. 3.16.

Based on the results of this test series, the fatigue behavior of fillet welded attachments with a 4 in. circular transition and the weld end ground smooth is adequately described by Category D.

3.2.2 Beams With Plates Intersecting the Webs

3.2.2.1 Crack Initiation and Growth

All beams tested in this series (W series) failed as a result of fatigue cracks which initiated at the toe of the fillet weld at either end of the plate piercing or butting against the beam web. Cracks grew vertically upward and downward from the initiation site in the beam web. One crack, typical of the type observed in these tests, is shown in Fig. 3.17.

As stated above, all cracks causing failure initiated at the toe of the fillet weld in the beam web. No slag inclusions were observed in any of the crack surfaces which were opened up. Some of the crack surfaces had a stepped appearance as shown in Fig. 3.18. This relief in the crack surface results when cracks initiate at more than one flaw simultaneously. These individual cracks then merge and propagation continues on a single crack front.

Cracks causing failure in this test series went through three phases of growth before the failure criterion was reached. The three phases were the same as described in Section 3.2.1.1 for the T and RG test series.

There were no other cracks observed in the beam web or flanges, or the intersecting plates.

3.2.2.2 Effect of Stress Range

As expected, the stress range had a pronounced effect on the fatigue life of each beam tested. In all cases, the minimum extreme fiber stress was kept constant and only the stress range was varied. The fatigue life decreased as the stress range was increased.

The test results for the W series of beams are presented in Table 3.3 and individual data points are plotted in Fig. 3.19. Some of the data points were obtained by repairing a crack and continuing testing to obtain a crack at the other end of the detail.

A regression line analysis was carried out on the 14 data points using the linear

model Log N = A + B Log S_r . This line is shown in Fig. 3.19. The equation for the life of a cover plated beam is also shown in the figue.

No fatigue cracks were observed at any location in specimen 1W. This beam was tested at a stress range of 5 ksi and over 15,000,000 cycles of load were applied. It is believed that this stress range must be very close to the fatigue limit for this particular detail.

3.2.2.3 Effect of Passing the Plate Through the Beam Web

Each beam tested in the W series consisted of two web details. In one detail (detail A), a 12 in. long plate passed through the beam web and in the other detail (detail B) two 6 in. long plates butted against the web on both sides of the beam.

Based on the number of data points obtained, no significant difference in fatigue life between piercing the web or butting up against the web was observed. In most beams tested, fatigue cracks grew simultaneously at both details.

3.2.2.4 Effect of Web to Plate Thickness Ratio

In this test series specimens 1W, 2W and 3W had a plate to web thickness ratio of 2.51 and specimens 4W, 5W and 6W had a plate to web thickness ratio of 3.26. The plots of regression line analyses on the data for the two plate to web thickness ratios are shown in Fig. 3.20.

Based on the data obtained in this test series, the plate to web thickness ratio does not appear to have a significant effect on the fatigue life of the detail.

3.2.2.5 Comparison With Previous Studies

The type of detail tested in this study, where one member intersects the web of another member, is not explicitly typified in the CSA design specification. If this detail is taken to be a fillet welded connection, then it would be classified as Category E. The fatigue behavior observed in the test series was compatible with Category E. The fatigue life was also compatible with results obtained by Bardell and Kulak from tests of beams with 90-degree transition attachments (11).

A number of tests of this type of detail have been carried out by Fisher et al. (22). The test series was prompted by failures on the Dan Ryan Expressway in Chicago . In the study, 2 in. thick plates were used and these were passed through a 0.8 in. thick web. This gave a plate to web thickness ratio of 2.50. A fillet weld was provided on one side of the web only. The test results obtained by Fisher are plotted in Fig. 3.20 along with the results of the W test series. The low fatigue life observed was attributed to large unfused areas which occurred under the fillet weld at the end of the plate.

All data points in the W test series, except one, fell above the confidence line for 95% survival obtained from tests on cover plated beams (3). This line is used as the basis for Category E in the CSA S16.1 Standard.

Based on the testing carried out, it seems reasonable to classify this type of detail

as fatigue Category E. However, it must be noted that no unfused areas were observed under the fillet welds at the ends of the plates in this study. In the study carried out by Fisher, this was not the case. This comparison of the study carried out by Fisher, and the study presented herein leads to speculation that the fatigue life of this type of detail may be influenced by the fillet weld size to plate thickness ratio, rather than the plate to web thickness ratio.

3.3 Fracture Mechanics Analysis of Test Specimens

3.3.1 General Background on Fracture Mechanics

The three stages which occur in the fatigue life of a structural member are fatigue crack initiation, fatigue crack propagation, and final failure (4,23). Any analysis using fracture mechanics deals with the life involved in the second phase, namely, fatigue crack propagation.

Fatigue crack initiation is generally not a concern in the fracture mechanics study of the fatigue life of a structural member. Studies have shown that all welded structural members have internal flaws or discontinuities present. The size and type of flaw which exists is a function of the type of detail, materials used, and fabrication procedures. Fatigue cracks initiate at these flaws. Maddox (24), and other researchers, have pointed out that the number of cycles required to initiate fatigue cracks at these flaws is so small that the initiation process may be safely ignored.

The final stage in the fatigue life of a structural member is also not considered in a fracture mechanics analysis. When the final failure stage is reached, the crack may have grown sufficiently large to cause yielding of the member, initiate brittle fracture, or cause excessive deflection and/or vibration. When any of these occur, the crack is likely growing at a rapid rate, and information concerning the growth rate and crack size will be of little practical use. All that remains, then, is to determine the size of the initial crack, and to establish how many cycles of load it will take to grow the crack from initial size to final failure size.

Thus, fracture mechanics is concerned with fatigue crack propagation. The fatigue life of a structural member may be predicted on the basis of initial crack size, stress range, and type of detail, using fracture mechanics.

Many forms of crack propagation laws have been proposed in the literature (25). These laws all relate the crack size to the number of load cycles with the stress range and a material constant.

These propagation laws may be written as:

$$\frac{da}{dN} = f(\sigma, a, B) \tag{3.1}$$

where:

a = crack size
N = number of load cycles
σ = stress range
B = a material constant

Paris (25) has proposed that macro-crack propagation is governed by the following equation:

$$\frac{da}{dN} = C(\Delta K)^n \tag{3.2}$$

where:

C = constant of proportionality of crack growth
K = stress range intensity factor
n= constant

The stress intensity factor, K, characterizes the stress field ahead of the sharp crack tip (1). It is linearly related to the nominal stress present in the structural member (σ), and the size of the crack which exists (a). The expression for K may be written as:

$$K = \sigma f(a) \tag{3.3}$$

More specifically, Irwin (26) has developed a general form for the stress intensity factor. The expression is as follows:

$$K = f(g)\sigma\sqrt{a} \tag{3.4}$$

In Equation 3.4, the term f(g) is a parameter that depends on crack geometry and type of detail. Equations 3.2 and 3.4, which are the framework of the fracture mechanics approach, can be shown to give a linear relationship between log of stress range and log of number of cycles. This relationship, Log N = Log M - n Log S_r , is consistent with test data. If Equation 3.4 is substituted into Equation 3.2, the result is:

$$\frac{da}{dN} = C\,[\,f(g)\Delta\sigma\sqrt{a}\,]^n \tag{3.5}$$

To determine the number of stress cycles to failure Equation 3.5 is integrated between the limits of crack size at initiation, a_i , and crack size a_i failure, a_f . Integration gives:

$$N_f - N_i = \frac{1}{C}\left[f(g)^{-n}\,\Delta\sigma^{-n}\,\frac{a^{1-n/2}}{1-n/2}\right]_{a_i}^{a_f} \tag{3.6}$$

The term $N_f - N_i$ gives the number of load cycles, N, which will cause the crack to grow from a_i to a_f . Calling this term N, and calling $n/2 - 1 = m$, Equation 3.6 can be written as:

$$N = \frac{1}{C}\,[\,f(g)^{-n}\,\Delta\sigma^{-n}\,]\,(a_i^m - a_f^m) \tag{3.7}$$

The crack size at failure will be much greater than the crack size at initiation. For positive m values, the term a_f^m may therefore be neglected. This gives:

$$N = \frac{1}{C}\,[\,f(g)^{-n}\,\Delta\sigma^{-n}\,]\,a_i^m \tag{3.8}$$

The term $\Delta\sigma$ is the algebraic difference between the maximum and minimum stress at the detail. In the analysis of structural details this is assumed to be constant and is expressed as the applied stress range, S_r . The terms in parentheses in Equation 3.8 will all be constant for a given material, geometry, and crack size and may be expressed as M. This gives:

$$N = M\,S_r^{-n} \tag{3.9}$$

This expression can be written in logarithmic form as:

$$\text{Log}\,N = \text{Log}\,M - n\,\text{Log}\,S_r \tag{3.10}$$

Equation (3.10) may be compared to the equation used in the linear regression analysis of the test data in Section 3.2 of this report. That equation was
$\text{Log } N = A + B \text{ Log } S_r$.

Thus, the fracture mechanics approach to the analysis of crack propagation leads to an exponential equation of a similar form as the equation empirically derived from the test data.

3.3.2 Fracture Mechanics Analysis of Members With Plates Intersecting the Webs

In this section, a fracture mechanics analysis will be used to give an estimate of the fatigue life of a structural detail. For purposes of illustration, the analysis will be carried out using members with plates intersecting the webs as the detail. This analysis will not be completely rigorous due to the fact that a finite element analysis is required to evaluate some of the variables involved; this is considered to be beyond the scope of this report. This section is presented to demonstrate the techniques used to apply fracture mechanics to welded joints and, in particular, to show how fracture mechanics can theoretically predict the fatigue life of welded details.

As stated previously, fracture mechanics is concerned with the second stage of fatigue life, fatigue crack propagation. This stage involves propagation from an initial crack size, a_i , to a final crack size, a_f . The ratio of a_i / a_f is small, such that the value of a_f is not a concern of the analysis. The number of cycles spent in the crack propagation stage is influenced by (27):

a. Rate of propagation
b. Size of the initial defect
c. Shape of the crack front

In order to evaluate fatigue life, a number of variables in the crack propagation equation must be evaluated. The value of the constant, n, in Equation 3.2 has been found to be 3.0 for ferrite-pearlite steels (1). Substituting this value, the crack propagation equation can be written as:

$$\frac{da}{dN} = C(\Delta K)^3 \tag{3.11}$$

The variables in this equation will now be examined in turn.

The detail under consideration in this section is a fillet welded joint, with non-load-carrying fillet welds. At this detail cracks initiate from flaws which occur at the toe of the fillet weld. These flaws may be in the form of slight undercut, sharp discontinuities, and/or slag inclusions. These types of defects have been analysed and measured by Signes et al. (28) and more recently by Watkinson et al. (29). Signes found that initial defect size varied from 0.0075 in. to 0.17 in. in depth, with an average size of 0.003 in. Watkinson found that the maximum depth of an initial defect, combining undercut

and inclusions, was 0.016 in. Watkinson also tested specimens with an artificially introduced notch at the fillet weld toe with a depth of 0.005 in. and a root radius of 0.0005 in. These tests fell within the scatterband of results conducted on as-welded specimens, demonstrating clearly that in as-welded specimens the weld defects are of this same size and type.

The crack propagation constant, C, has been determined experimentally by many researchers. Barsom (30) gives a C value of 3.6×10^{-10} for ferrite-pearlite steels. Hirt and Fisher (31) have determined a C value of 2.05×10^{-10} . The value given by Barsom is an upper bound value and is intended to be used for design, rather than to predict test results. Fisher et al. (4) and Slockblower and Fisher (32) have found that a C value of 2.0×10^{-10} provides good correlation with test results. Rolfe and Barsom (1) have reported that the value of C in the heat affected zone is equal to or less than in the base metal. A value of $C = 2.0 \times 10^{-10}$ will be used in this analysis. All of the values for C referred to herein are for crack size (a) in inches and stress range intensity factor (K) in ksi in.

The size of the initial crack, and the shape of the initial crack both have an influence on the stress intensity factor, K. As the crack propagates through the plate thickness the value of K changes. However, the change is not great and its effect will not be included in this analysis. The value of K will be determined after the manner of Maddox (33). Maddox has proposed that for fillet welded joints, the solution of the stress intensity factor for a surface crack may be written as:

$$K = \frac{M_s M_t M_p M_k}{\phi_0} \sigma \sqrt{\pi a} \qquad (3.12)$$

where:

M_s = free surface correction
M_t = finite plate thickness correction factor
M_p = correction factor to allow for the plastic zone at the crack tip
M_k = magnification factor showing the influence of geometric stress concentration
ϕ_0 = complete elliptic integral

The free surface correction factor, finite plate thickness correction factor, and the complete elliptic integral are all functions of the ratio of crack depth, a, to crack width, 2b. This ratio varies only slightly as the crack propagates through the plate thickness. The value of a/2b has been studied extensively by several researchers for cracks originating at fillet weld toes (3,4,32,33,34). A value of $a/2b = 0.67$ is consistent with the findings of researchers for the usual range of crack depths observed. Maddox (33) gives a value of $M_s M_t / \phi_0$ as 0.815 for a ratio of $a/2b = 0.67$.

The influence of the crack tip plasticity correction factor, M_p , is small for fatigue crack propagation under elastic stresses (33). For this analysis a value of 1.0 will be used for M_p .

The magnification factor M_k , is largely a function of the geometry of the fillet welded joint. This is perhaps the most difficult factor to evaluate. Indeed, as Albrecht and Yamada (35) have pointed out, the present classification of structural details by categories in current fatigue design specifications is essentially a classification by the severity of local stress gradients.

Recently, solutions for M_k have been presented in the literature based on various finite element techniques (4,27,32,33,35,36). These solutions deal mainly with fillet welds at the end of cover plates, attachments fillet welded to a beam flange, or fillet welds on both sides of a vertical stiffener. Solutions for horizontal attachments welded to a beam web are not available. However, it is felt that the values of M_k given for non-load-carrying fillet welds (as in the case of a vertical stiffener) provide a good estimate of M_k for horizontal attachments.

The value of M_k used is influenced by the angle of the weld material to the plate, depth of the fatigue crack or initial flaw, plate and attachment thicknesses, fillet weld leg length, and length of attachment. Because M_k is a function of all these variables, some randomized by the welding process, determination of an absolute value of M_k for the detail being considered is beyond the scope of this study.

In the literature, values of M_k ranging from 2.0 to 7.3 have been reported. Values of 2.0 to 4.0 are those cited for non-load-carrying fillet welds. Gurney (27) has suggested that part of the discrepancy in the determination of M_k lies in the mesh size used in the actual finite element analysis of the joint. He also states that after the crack has propagated through 35% of the plate thickness the effect of M_k becomes negligible. Fisher et al. (4) agree with this concept and use a decay constant in evaluating the stress intensity factor. In this study the influence of stress concentration will be included by using a value of M_k = 3.0.

The equation of crack propagation may now be written as:

$$\frac{da}{dN} = C\left[\frac{M_s\, M_t\, M_p\, M_k}{\phi_0}\,\sigma\,\sqrt{\pi a}\right]^3 \tag{3.13}$$

Substituting the previously mentioned values and calling $\sigma = S_r$ gives:

$$\frac{da}{dN} = (2.0\text{x}10^{-10})\,[(0.820)(1.0)(3.0)(S_r\,\sqrt{\pi a})]^3 \tag{3.14}$$

Performing the integration, the expression may be written:

$$N = (1.229\text{x}10^{8})(a^{-0.5})(S_r^{-3}) \tag{3.15}$$

This equation is plotted (along with the test data) in Fig. 3.21 for initial crack sizes of 0.004, 0.007 and 0.03 in. An initial crack size of 0.004 in. provides a good upper bound to the test data, while an initial crack size of 0.03 in. provides a lower bound to the test data.

The average initial crack size, based on the experimental data, is 0.007 in. This average initial crack size is approximately twice as large as the average initial defect size reported by Signes et al. Maddox (24) has also noted that an initial defect size of 0.003 in. is smaller (by a factor of 3.5) than the initial crack size, a_i , which he used in the crack propagation equation to obtain results consistent with test data. This leads to the possibility that even for welded joints with relatively large defects, there is a small crack initiation stage in the life of the joint. Gurney (27) has also noted the existance of an initiation period and suggests that it decreases with increasing stress gradient. Roberts and Irwin (23) suggest that the end of this crack initiation period is reached when a crack is growing at a rate of 10^{-7} in./cycle. By comparison, they also suggest that the end of the crack propagation stage occurs at a growth rate of 10^{-4} in./cycle. If the average initial crack size in this test series was less than 0.007 in., then the rate of fatigue crack propagation value (C), or the effective stress intensity value (K), would have to be increased.

One other factor must be considered when comparing the fracture mechanics analysis with the test results. The fracture mechanics approach predicts the number of cycles required for the crack to propagate through the plate thickness, or in this case the beam web. However, in the test series the failure criterion was reached at a later stage than this. Thus, the fracture mechanics predictions slightly underestimate the observed fatigue lives.

TABLE 3.1 Summary of Test Results

Tapered Transition Bracing Attachment

Specimen	Stress Range (ksi)	Crack First Observed (cycles)	N Failure (cycles)
1T	11	727,500	874,500
1T	11	727,500	987,600
2T	17	108,000	229,500
2T	17	108,000	229,500
1TG	11	225,000	1,162,500
1TG	11	577,500	1,753,500
P1	13	-	714,000*
P2	13	-	744,000*

* = From Pilot Test (Ref. 11)

TABLE 3.2 Summary of Test Results

Circular Transition Bracing Attachment

Specimen	Stress Range (ksi)	Crack First Observed (cycles)	N Failure (cycles)
1RG	11	738,000	1,329,000
1RG	11	-	2,240,000*
2RG	13	487,500	1,336,500
2RG	13	487,500	1,387,500
3RG	17	111,000	432,000
3RG	17	213,000	498,000
4RG	10	2,262,000	3,741,000
4RG	10	-	8,086,000*
5RG	15	-	FVS
6RG	19	-	505,500
6RG	19	-	844,500

* = Test Discontinued Before Crack Observed
FVS = Failure Occured at Vertical Stiffener

TABLE 3.3 Summary of Test Results

Beams With Plates Intersecting the Webs

Specimen	Stress Range	Crack First Observed (cycles)	N Failure (cycles)	Type of Detail
1W	5	-	15,931,000*	-
2W	10	610,500	1,441,500	A
2W	10	1,378,500	1,738,500	B
2W	10	1,378,500	1,813,500	A
2W	10	-	1,813,500	B
3W	15	231,000	357,000	A
3W	15	231,000	357,000	B
3W	15	231,000	357,000	B
4W	10	770,000	1,296,000	A
4W	10	-	1,821,000	B
5W	17	82,500	144,000	A
5W	17	-	222,000	B
6W	13	-	798,000	B
6W	13	-	798,000	B
6W	13	-	798,000	A

* = Test Discontinued Before Crack Observed

A = Plate Passing Through Web

B = Plate Interrupted at Web

Figure 3.1 Tapered Transition Bracing Attachment

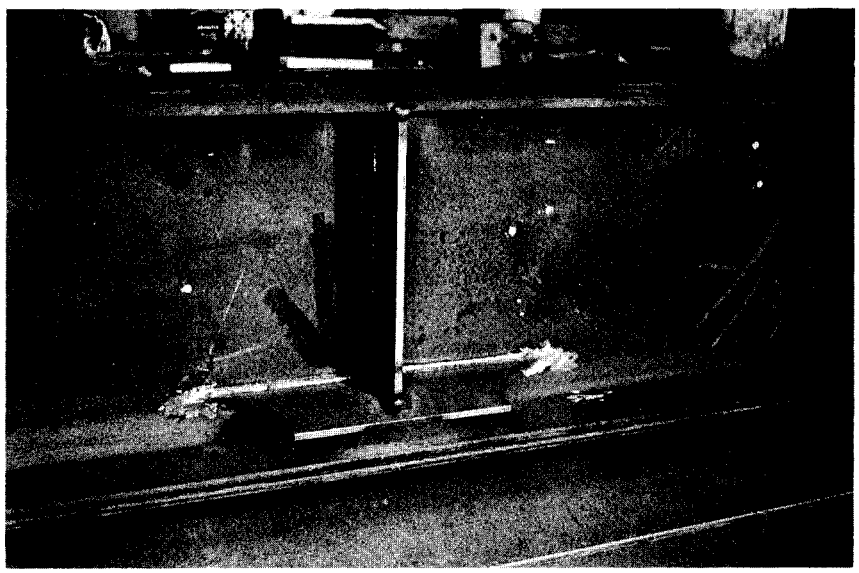

Figure 3.2 Circular Transition Bracing Attachment

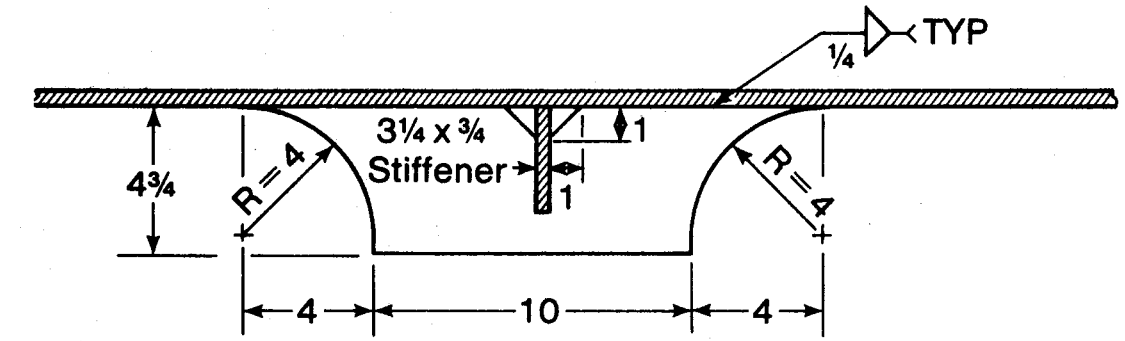

Section A-A

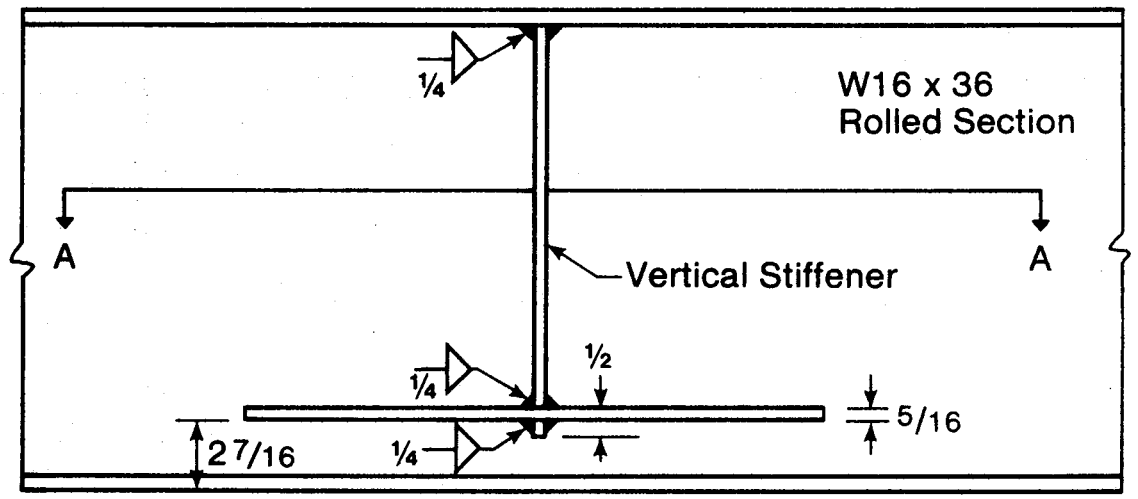

Figure 3.3 Tapered Transition Bracing Attachment Detail

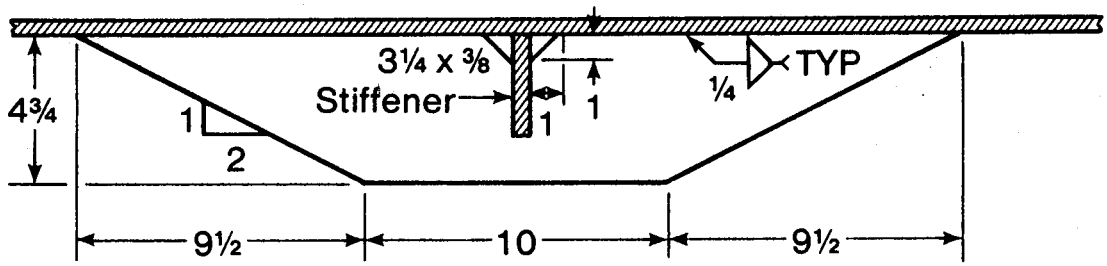

Section A-A

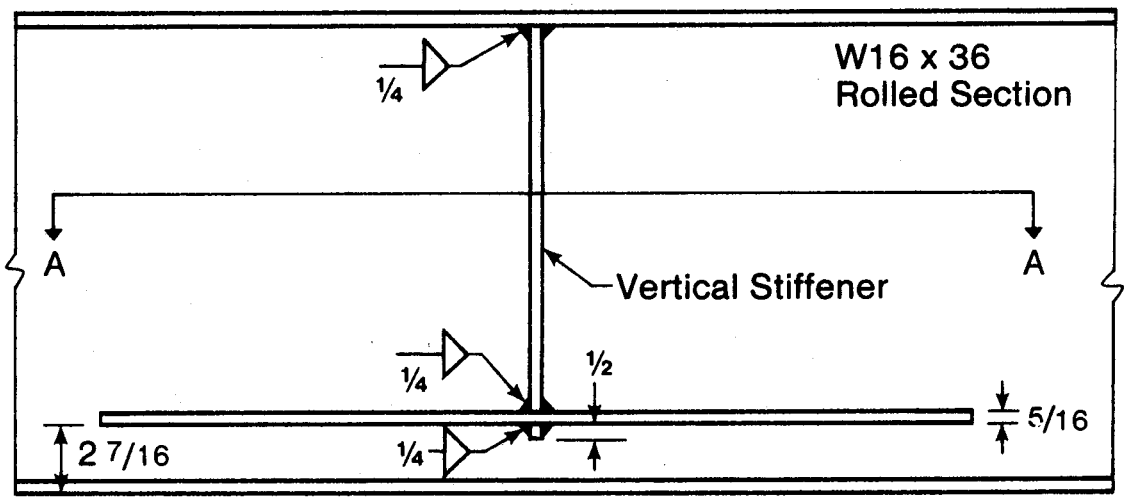

Figure 3.4 Circular Transition Bracing Attachment Detail

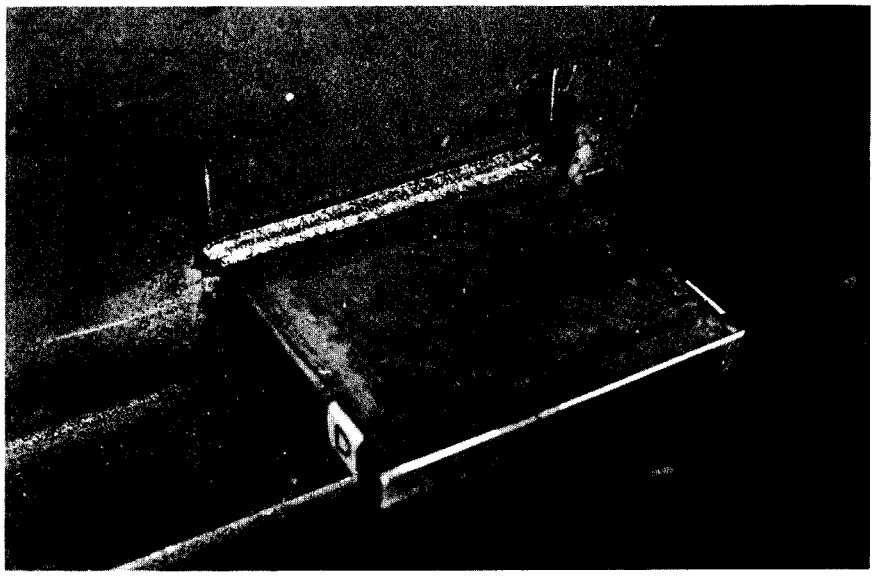

Figure 3.6 Crack at End of Tapered Attachment

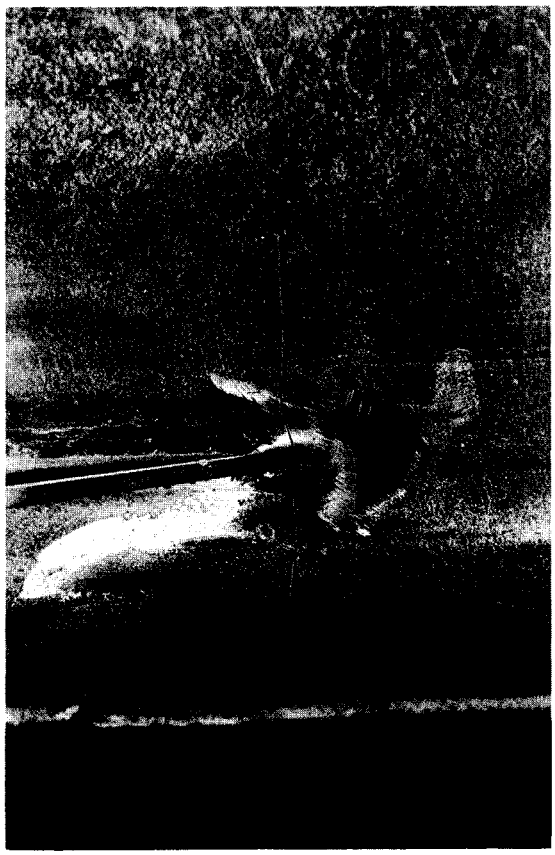

Figure 3.5 Beam With Plate Intersecting the Web

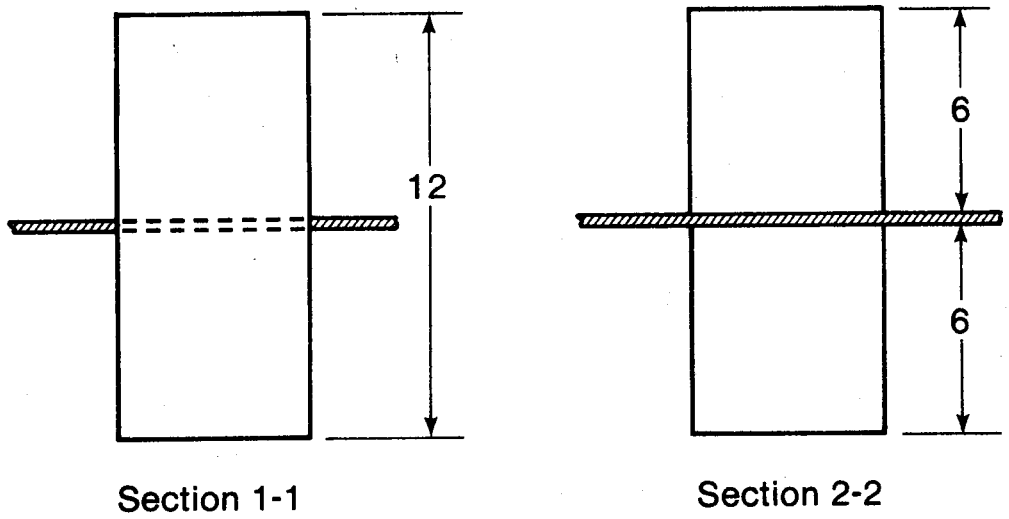

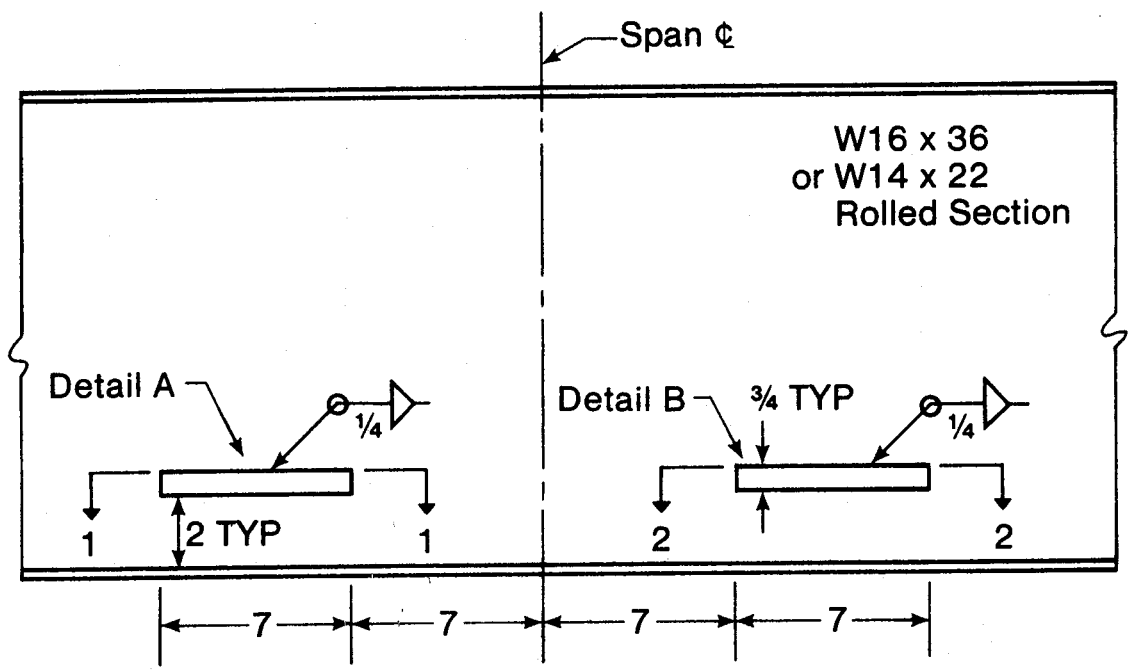

Figure 3.7 Details of Plates Intersecting the Web

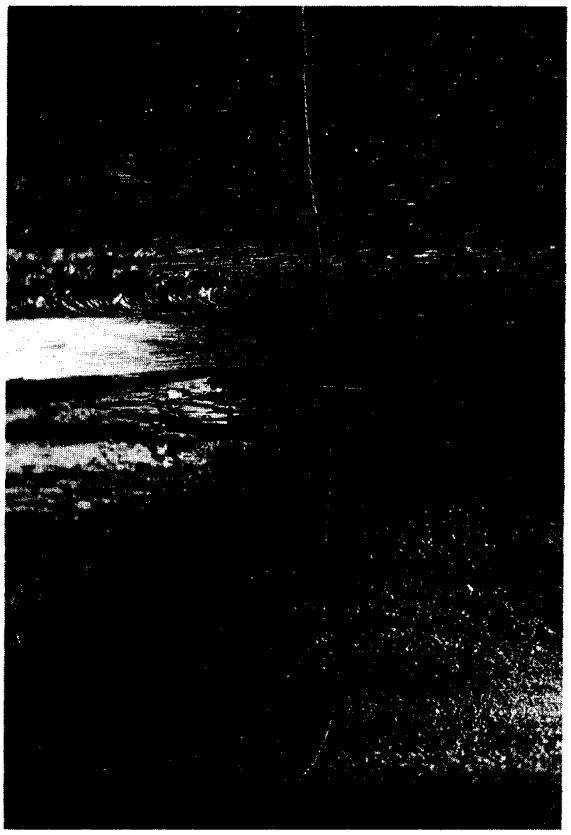

Figure 3.8 Crack at End of Circular Transition Attachment

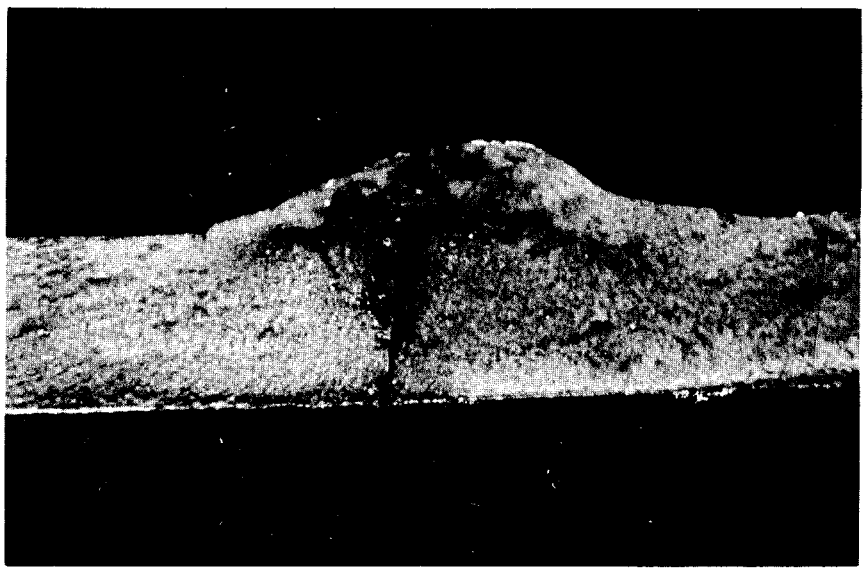

Figure 3.9 Fracture Surface of Crack

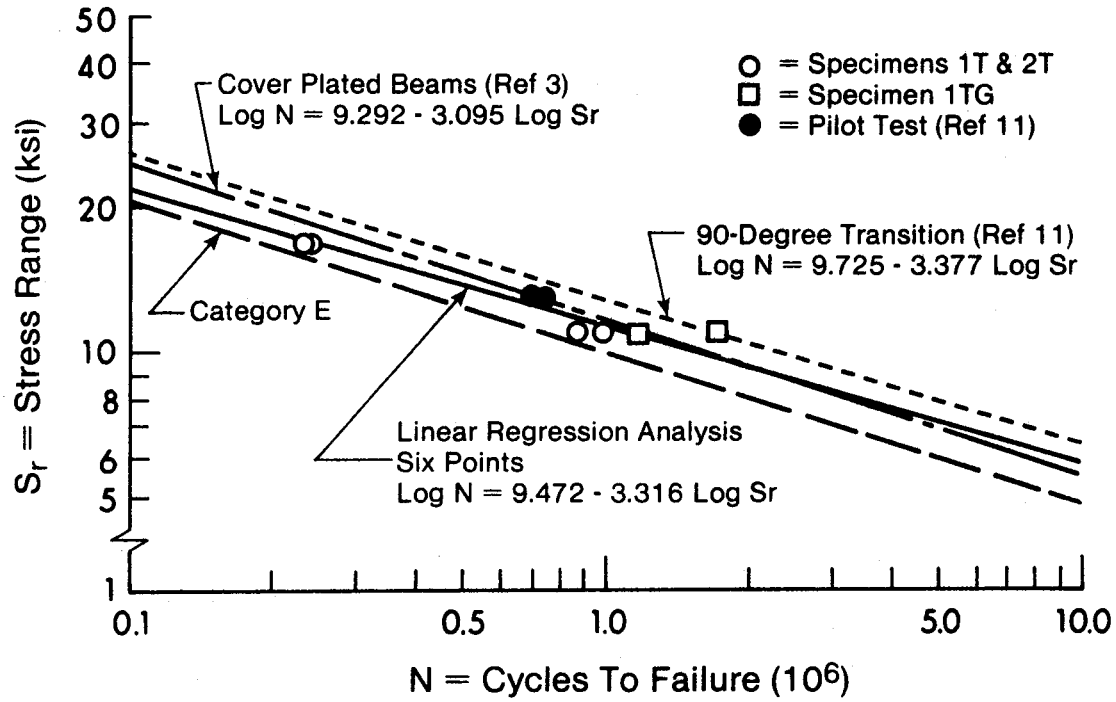

Figure 3.10 Beams With Tapered Bracing Attachments

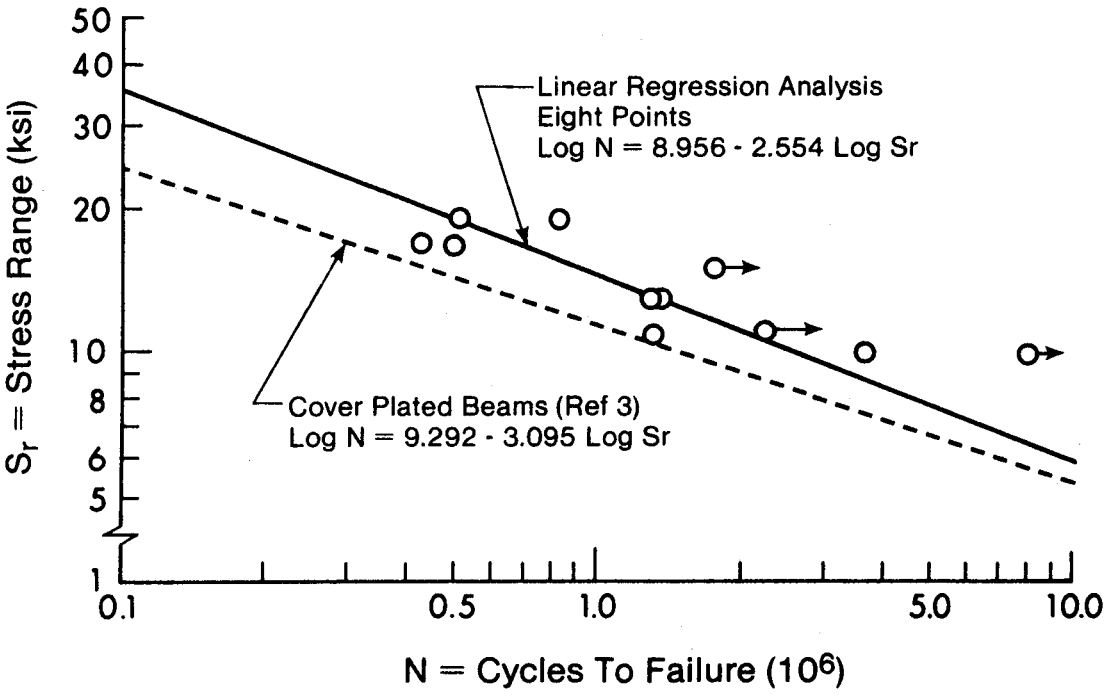

Figure 3.11 Beams With Circular Transition Attachments

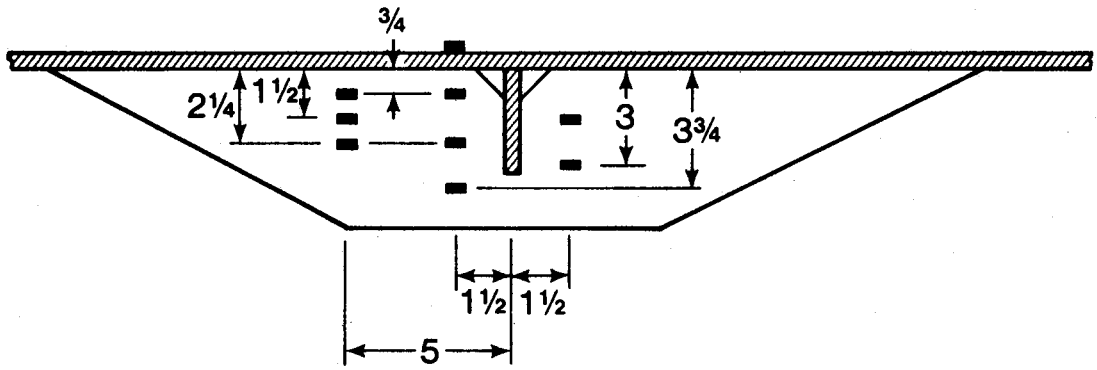

Figure 3.12 Strain Gauge Locations on Tapered Attachment

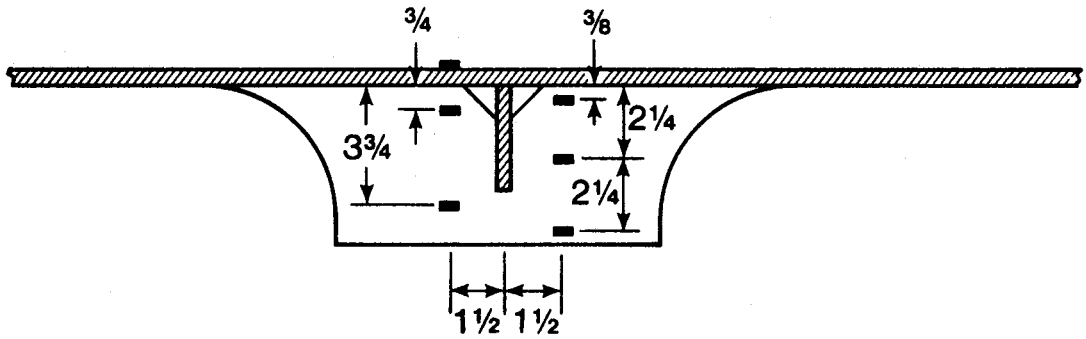

Figure 3.13 Strain Gauge Locations on Circular Transition Bracing Attachment

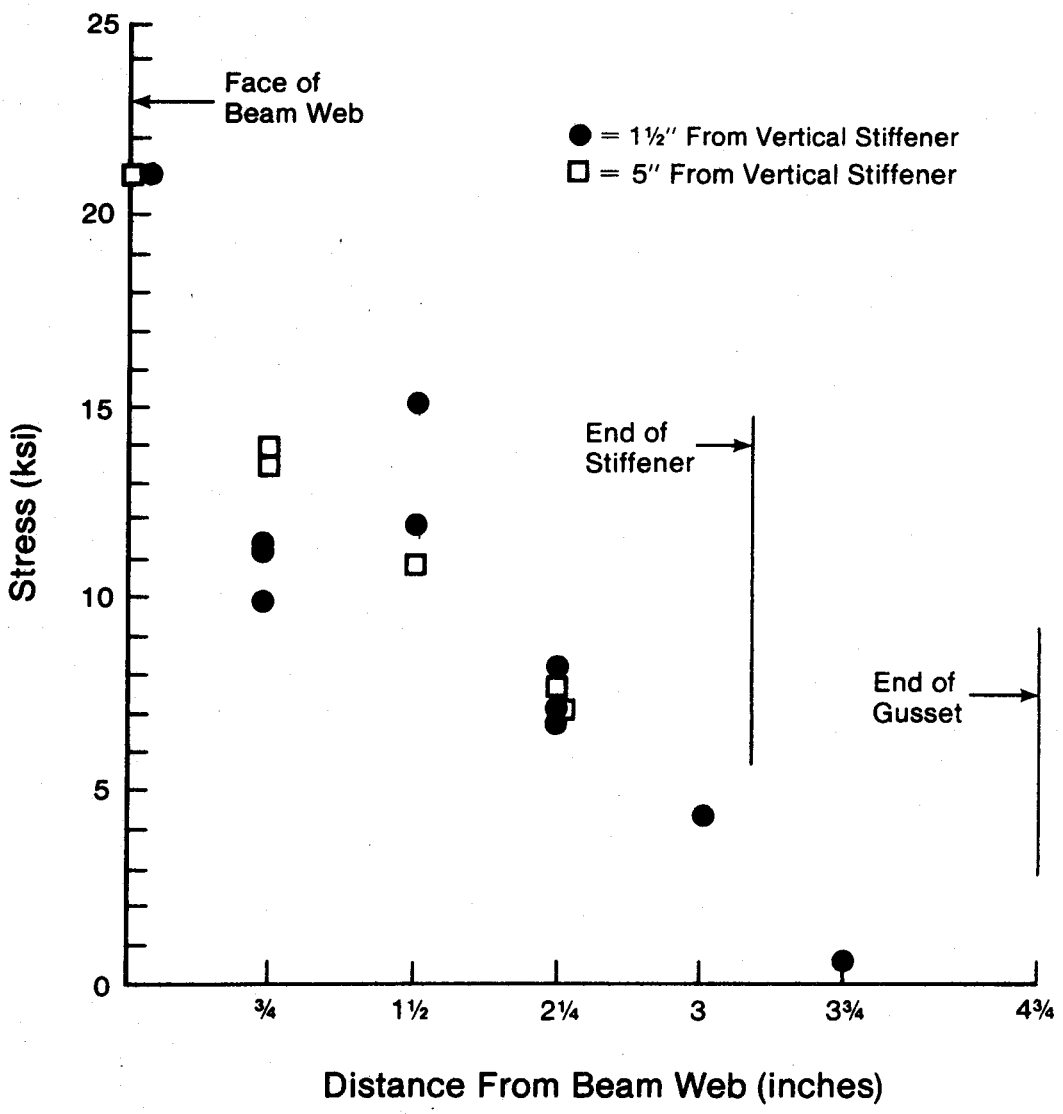

Figure 3.14 Stress Distribution in Tapered Attachment

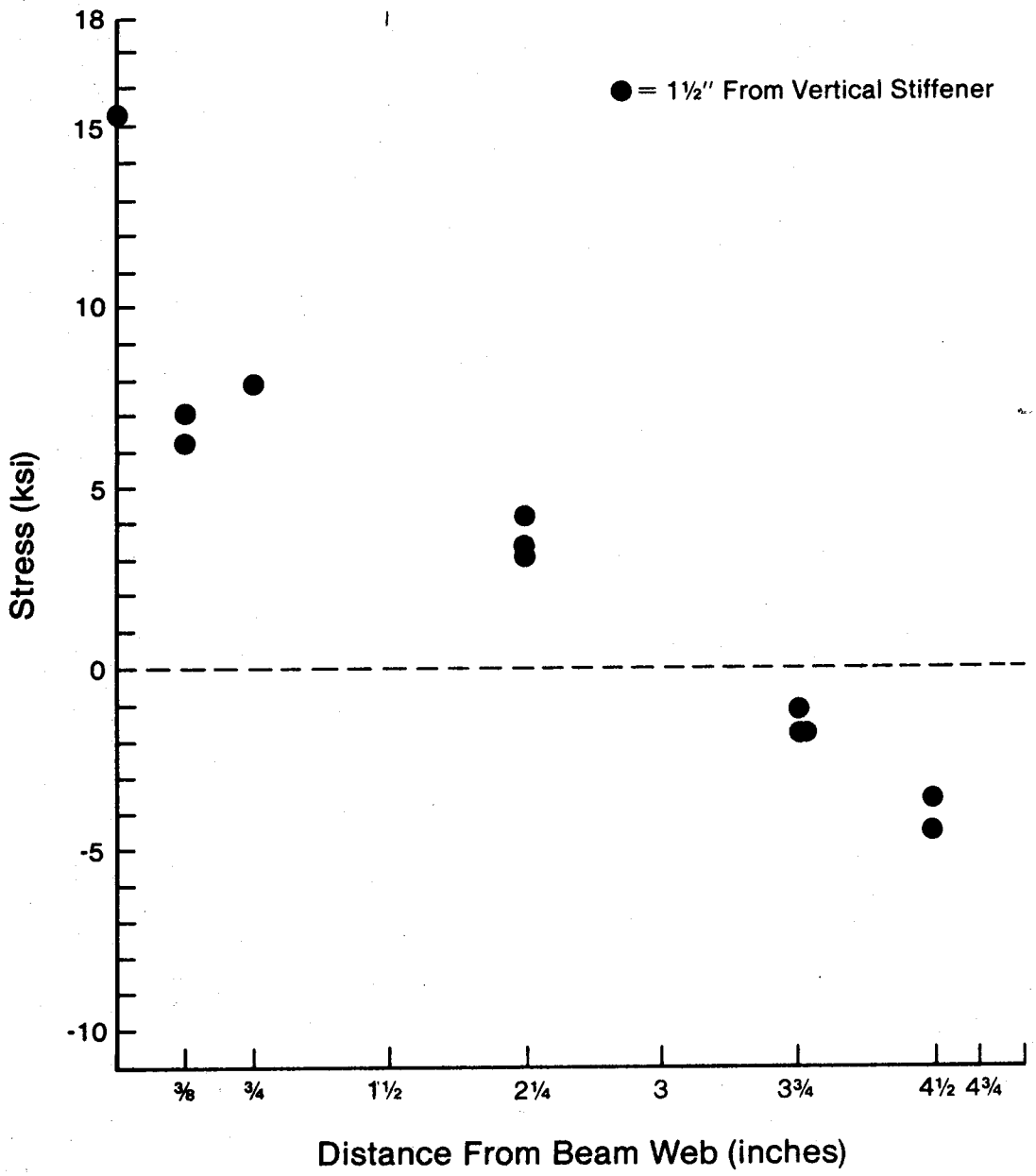

Figure 3.15 Stress Distribution in Circular Transition Attachment

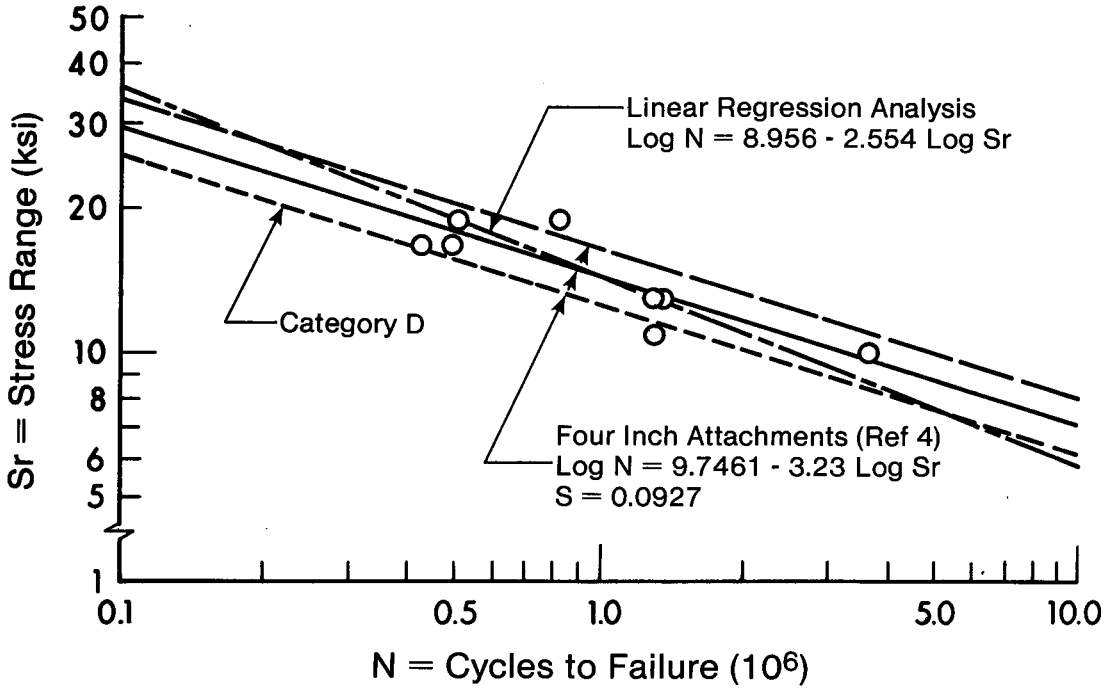

Figure 3.16 Circular Transition Series Results Compared With CSA Category D

Figure 3.17 Crack in Beam With Plate Piercing Web

Figure 3.18 Fracture Surface of Crack

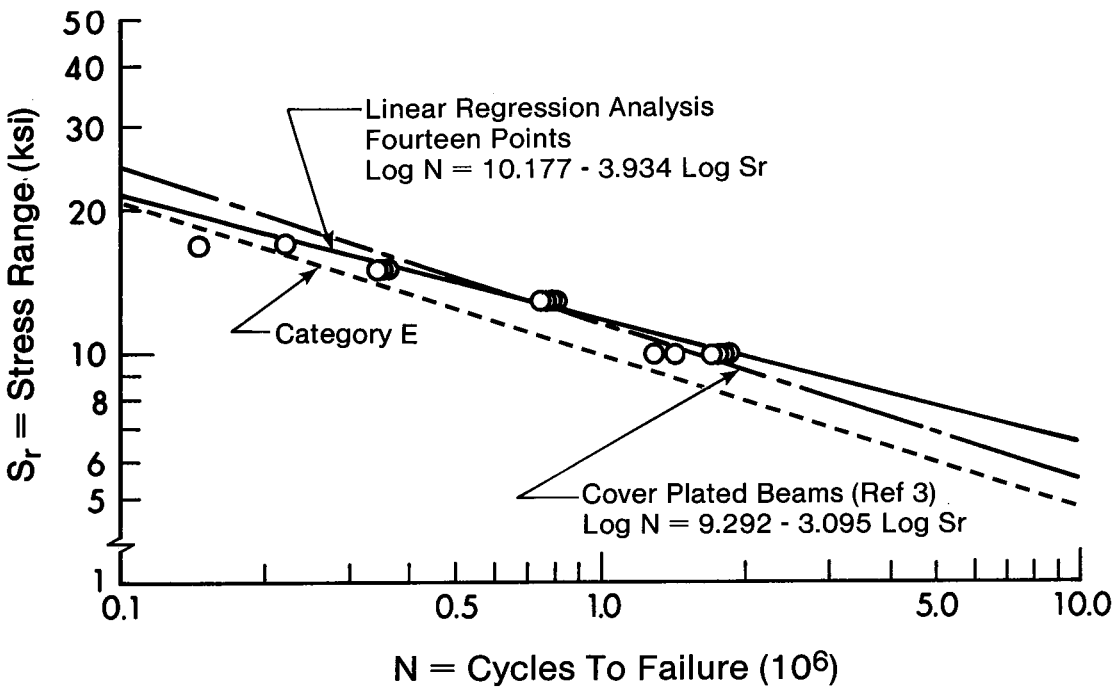

Figure 3.19 Beams With Plates Piercing the Web

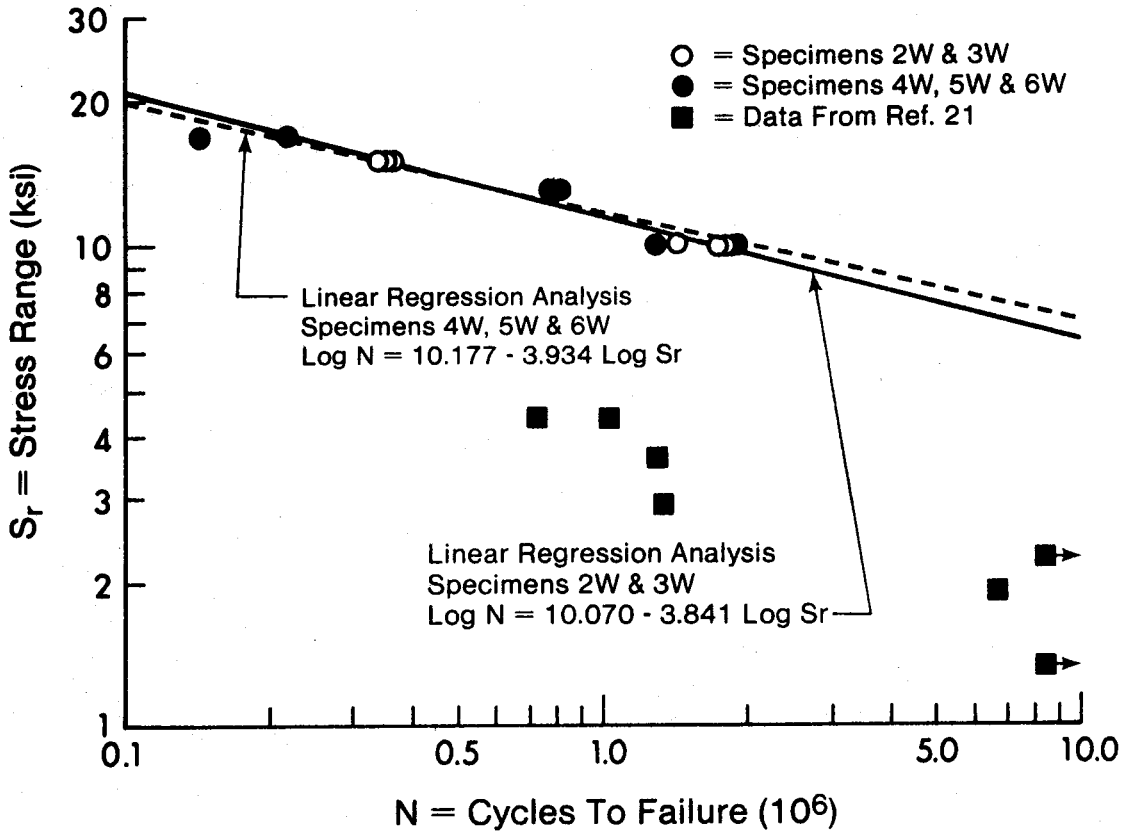

Figure 3.20 Effect of Plate to Web Thickness Ratio

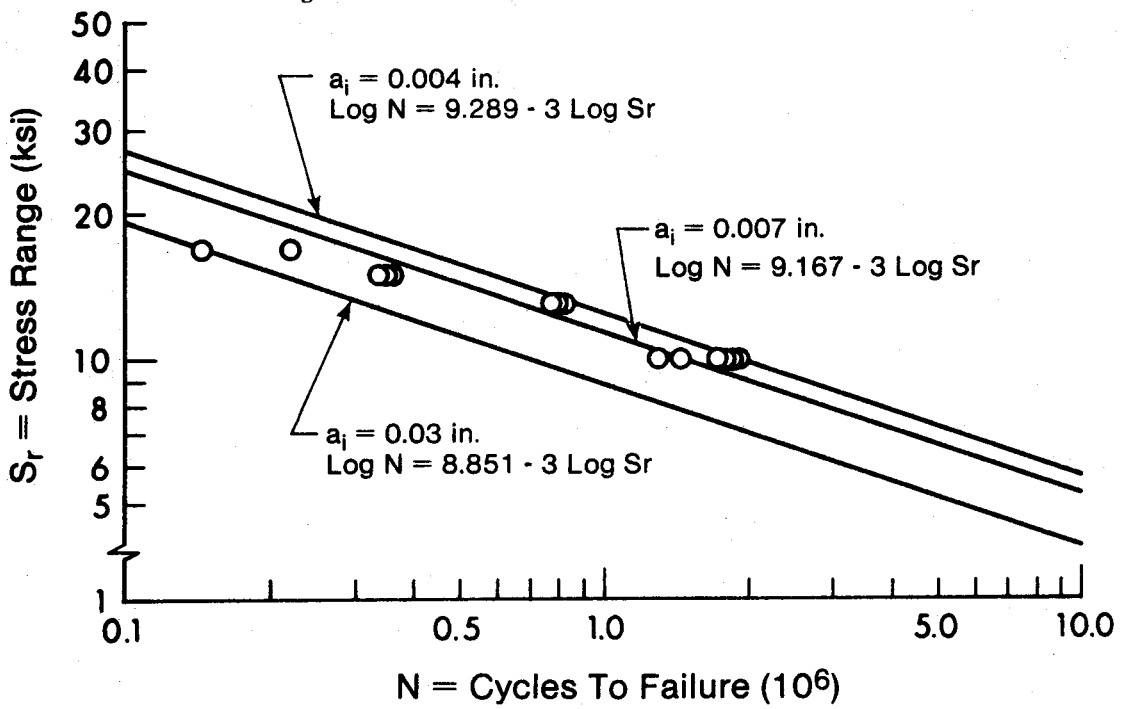

Figure 3.21 Fracture Mechanics Analysis Results

4. PHASE II - HSS TRUSSES WITH WELDED CONNECTIONS

4.1 Experimental Program

4.1.1 Scope

Primarily as a pilot study, four tests were conducted to investigate the fatigue strength of trusses made up of hollow structural sections (HSS), with welded connections. The purpose of the study was to compare the fatigue life of an actual truss to the presently available design recommendations (5,6,7,19).

All four trusses tested had the overall dimensions and layout as shown in Fig. 4.1. The K-joint at mid-span on the lower chord was considered to be the principal joint under investigation, although two of the trusses subsequently failed at joint U2. The K-joint was designed with a 40% overlap in all four trusses. The definition of overlap and details of this joint are shown in Fig. 4.2. Joints U1 and U2 were designed with a 54% overlap in truss specimen T1F, and a 62% overlap in truss specimens T2F, T3F, and T4F. Details of these joints are shown in Fig. 4.3. Based on previous tests of isolated joints (12,13,14), it was felt that the fatigue life of the trusses would be closely predicted by CSA Category E.

The design recommendations available at present are founded on tests of isolated HSS joints, and not on joints which have been tested as a part of a truss. However, in joint tests no secondary stresses are developed due to bending or deflection as in a truss. In addition, the joint specimens all had a pre-compressed chord member. In the truss test, the chord at the K-joint will be repetitively loaded in tension, resulting in a more severe (and realistic) fatigue situation.

4.1.2 Specimen Description

The four trusses used in this investigation were made up of HSS sections meeting the requirements of CSA G40.21 50W, Class H (21). Overall truss length was 14 ft.-3 1/4 in., and overall height was 4 ft.-8 in. The trusses were fabricated using normal shop practice by a local steel fabricator. All welds were done manually by the shielded-metal arc process, using AWS E7018 electrodes. Prior to final welding, the locations of all tack welds were recorded.

At joint L1, the center K-joint, a combination of fillet and groove welds were used as shown in Fig. 4.2. The groove weld was to be full penetration, with a back-up bar. In fabrication, the groove weld was placed on the joint first, then the fillet weld was applied. All of the other joints in the truss had only fillet welds, and all welds were inspected visually prior to testing.

The upper and lower chords of the truss were filled with high strength (5000 psi), expanding grout at the reaction and load points for a distance of 18 in. in from the end of each member. This was done in order to prevent excessive flexing of the tube webs at points of concentrated loads, and also to prevent web crippling.

Truss T1F was made up of HSS 6 x 4 x .188 top and bottom chord members,

HSS 5 x 5 x .250 outer diagonal web members, and HSS 3-1/2 x 3-1/2 x .150 inner diagonal web members. Trusses T2F, T3F, and T4F were made up of HSS 6 x 4 x .250 top and bottom chord members, HSS 6 x 6 x .375 outer diagonal web members, and HSS 3-1/2 x 3-1/2 x .188 inner diagonal web members.

4.1.3 Test Set-Up

All trusses were tested on a 13 ft. span with the load applied at one of the upper chord panel points as shown in Fig. 4.4. The reaction nearest to the load point was simply supported on a steel rocker and the far reaction was a simply supported pinned end. During the test, lateral support was provided to the truss at both upper panel points.

An Amsler testing system, as described in Section 3.1.2.2, was used to apply the fatigue loading. The static and dynamic loads applied to the truss were identified in the same manner as described in Section 3.1.2.2. The strain gauges used to relate the static and dynamic loads were mounted at the center of each face of the inner diagonal tension member (L1 U2). Thus, the nominal stress in the member was used to determine the stress range during testing.

The four trusses in this test series were tested at a loading rate of 500 cpm.

4.1.4 Test Procedure

All four trusses were tested in a similar manner. In each case the minimum load on the truss was 10 kips. This provided a minimum stress of 1.5 ksi in member L1 U2 for truss T1F, and a minimum stress of 1.3 ksi in member L1 U2 for trusses T2F, T3F, and T4F. The stress ranges for the four trusses varied between 4.7 and 7.3 ksi, as related to member L1 U2.

The criterion used to determine failure of a truss was somewhat arbitrary. For this test series, failure was assumed to have occured when approximately one-quarter of the cross section of member L1 U2 had been eliminated from carrying load by fatigue crack propagation. This failure criterion also corresponded to a visible flexing at the crack. Because of the failure criterion selected, tests were carefully monitored and only conducted with an observer present.

Before testing was begun, shims were placed where required at both reaction points. This was done so that no bending was introduced into the web members during loading. Strain gauges were mounted at mid-length of members L0 U1 and L2 U2 on the faces parallel to the face of the truss. These gauges were used to determine how much shimming was required.

Trusses were loaded statically to obtain strain distribution and deflection readings before the fatigue testing was begun. After completion of fatigue testing, fatigue damaged areas of the truss were removed by flame cutting. The fatigue cracks were then saw-cut open and the fracture surfaces examined.

4.2 Test Results

4.2.1 Crack Initiation and Growth

Trusses T1F and T2F both failed as a result of cracks which initiated and grew in the region of joint L1. In trusses T3F and T4F the cracks causing failure initiated in the region of joint U2. All of the cracks contributing to the failure of each truss were at either end of the inside diagonal placed in tension by the applied load (L1 U2).

The fatigue cracks observed in specimen T1F started in the vertical groove weld at the intersection of members L1 U1 and L1 U2. On one face of the joint the crack grew vertically upward and downward from the initiation site. The lower crack front then propagated through the horizontal fillet weld and kept moving along the lower toe of this fillet weld as shown in Fig. 4.5. The upper crack front propagated along the horizontal edge of the groove weld as may also be seen in Fig. 4.5.

On the opposite face of the joint, the fatigue crack initiated in the vertical groove weld but grew in a direction perpendicular to the tension member, which is the member on the left in Fig. 4.6. The lower crack front propagated along the top of the horizontal fillet weld and the upper crack front propagated horizontally along the edge of the groove weld. Both of these later stages of crack growth may be seen in Fig. 4.6.

In truss T2F cracks also initiated on both faces of joint L1. On one face, initiation occurred in the vertical groove weld and the crack propagation pattern was virtually identical to the pattern of the first crack described for specimen T1F (Fig 4.5). On the opposite face of this joint, no cracks initiated in the vertical groove weld. One crack initiated at the toe of the horizontal groove weld, at the outside corner of the tension diagonal. This crack then propagated simultaneously along the edge of the horizontal groove weld and across the face of the diagonal tension member as shown in Fig. 4.7. The crack was nearly perpendicular to the longitudinal axis of the diagonal member on the vertical face.

Two other cracks were also observed on the opposite face of this joint. Both were in identical locations, at the toe of the horizontal fillet weld at the corner of the joint between the diagonal member and the top of the lower chord. One such crack, at the end of the diagonal in tension, may be seen in Fig. 4.8 (above the arrow on the photograph). The crack at the end of the tension diagonal kept propagating during the entire testing period, while the crack at the end of the compression diagonal stopped growing after reaching a length of approximately 1/2 in.

Trusses T3F and T4F both failed as a result of fatigue crack propagation at the top of member L1 U2. In both of these trusses, cracks were observed on the two outside faces (faces parallel to the plane of the truss) of joint U2 as shown in Fig. 4.9. The surfaces of the cracks were stepped as shown in Fig. 4.10, indicating many initiation sites. (Fig. 4.10 is a photo of the underside of member L1 U2 at joint U2, in the region shown in Fig. 4.9. In Fig. 4.10 the horizontal fracture surface was located along the end of member L1 U2. The vertical weld bead shown was at the underside of member L1 U2, where it was welded to the upper chord). It is felt that the cracks initiated inside the joint and propagated along the weld metal to heat affected zone junction to the outside of the joint. This can be seen

in the crack profile shown in Fig. 4.11. (Fig. 4.11 is a section cut through one end of the crack shown in Fig. 4.9.) In each of these cases, the cracks initiated in the region where the fillet welds of member L1 U2 intersect those of member L2 U2. The cracks then grew simultaneously in both directions away from the initiation site and parallel to the direction of the weld material.

In truss T3F fatigue cracks were also observed at the toe of the fillet weld, on the two corners, of one face of joint L1, as described for T2F (Fig. 4.8). However, these cracks did not propagate through the wall thickness of the web or chord member before failure occurred at joint U2.

In truss T4F a fatigue crack was also observed at the toe of the fillet weld at one corner of joint L1, as described for specimen T2F (Fig. 4.8). However, as in specimen T3F, the crack did not propagate through the thickness of any member before joint U2 failed.

4.2.2 Effect of Stress Range

As expected, stress range was one of the main variables in governing the fatigue life of these trusses. This can be seen clearly in Fig. 4.12 where the nominal stress range in member L1 U2 is plotted against the number of cycles obtained in each test. An increase in the stress range resulted in a decrease in the number of cycles to failure of the truss.

Each data point in Fig. 4.12 represents one of the trusses tested. (Test results are also presented in Table 4.1.) The Figure shows that the fatigue lives obtained in the test series are significantly lower than would be predicted by Category E or Category F.

The four test points obtained are the result of failures at two different locations, joint L1 and joint U2. These locations are at either end of member L1 U2 and the same stress range would govern in the design of each joint. Although the two details are different, the scatter in the data points obtained is minimal. Based on the test results, these two details exhibit similar fatigue behaviour and could be classified in the same fatigue category.

A regression line analysis using the linear model $\text{Log } N = A + B \log S_r$ was carried out on the four data points and is shown in Fig. 4.12. The equation obtained has a slope of -4.575 which is shallower than the slope of -3 obtained from tests on beam details (3,4). However, this slope is consistent with slopes obtained from test results of HSS joints presented in the STELCO design manual (19).

An analysis based on three data points, excluding truss T1F, is also shown in Fig. 4.12. The equation of the resulting linear model has a slope of -3.346. This is in reasonable agreement with the slope of -3 used by the present CSA design standards. Truss T1F is excluded from the analysis on the basis that the transverse stiffness (thickness/width ratio) of the joint members has been found to have an effect on fatigue performance (12). The wall thicknesses of the chord and web members at joint L1 in truss T1F are smaller than in trusses T2F, T3F and T4F.

4.2.3 Stress Distribution in Truss Members

As a part of the testing program, the stresses present in the truss members were monitored. Strain gauges were placed at mid-length of all members with one gauge at the center of each face of each member. Readings were taken at the maximum static load the testing machine could apply (approximately 100 kips). The averages of all the readings taken from specimens T2F, T3F, and T4F are given in Table 4.2. T1F is not included because of its different member dimensions.

The readings in Table 4.2 are compared to stresses obtained from an analysis of the truss using the Plane Frame and Truss Program (PFT) in the Department of Civil Engineering Computer Program Library. The analysis was carried out with a load of 96 kips applied at joint U1. The stresses from this analysis are consistent with those obtained experimentally from the trusses.

The member stresses determined by PFT shown in Table 4.2 were obtained assuming rigid joints in the truss. A similar analysis using pinned joints was also carried out. Whether pinned or rigid joints were assumed, approximately the same forces in the members were obtained. The maximum difference was a 3.4% increase (pinned vs. rigid), and the average difference was a 1.0% increase in member force.

4.2.4 Stress Distribution at K-Joint

Stresses at the K-joint (joint L1) were measured using strain gauges at various locations. As expected, it was found that high local stresses occur in the vicinity of the joint. These local stresses were found to be up to 2.6 times greater than the nominal stresses in the members meeting at that joint. The centerlines of the gauges used to measure these stresses were placed approximately 3/8 in. from the toe of the weld. It is considered that these stresses are probably even higher at the weld toe.

The stress distribution measured at the K-joint in specimen T2F is given in Table 4.3. The location of each gauge is shown in Fig. 4.13. These readings were taken with the maximum static load applied by the testing machine.

The highest local stresses were measured in the vicinity of the vertical groove weld at the top of the chord member. This is near the location of crack initiation in specimens T1F and T2F. Also, there are high local stresses around the horizontal groove weld. In specimen T2F a crack initiated in this region.

Stresses at the K-joint were also obtained using a finite element analysis. The results of this analysis are given in table 4.3. The calculated values obtained follow the same trend as the measured values. However, measured stresses at a number of the gauges were higher than the calculated values. This is probably due to the element size chosen for the analysis. The finite element technique used calculated stresses at the centroid of each element, and element centroids did not directly coincide with strain gauge locations. It is felt that if the element sizes are sufficiently small the analysis will reach the measured values. Also, the analysis used constant thickness elements, and thus did not incorporate the effects of the weld bead at the joint.

4.2.5 Comparison With Previous Studies

The fatigue lives observed in this test series are lower than the lives which would be predicted based on previous studies (12,13,14). However, as was stated earlier, previous studies concentrated on testing of isolated joints rather than entire trusses.

The design recommendations given for welded HSS connections (19) predict a fatigue life slightly higher than CSA Category E for joints with 100% overlap and slightly lower than Category E for joints with a 47% overlap. The failures observed in this test series had fatigue lives significantly lower than would be predicted by Category E or Category F. This can be seen in Fig. 4.12, where Category E and Category F are compared with the test results.

The difference between the truss test results and the results obtained from joint tests can be better understood by comparing the two types of test. During the joint tests the chord was pre-compressed at a constant load for the entire test period, while in the truss test both chord members are repetitively loaded, one in tension, the other in compression. Also, no secondary stresses are introduced due to bending or deflection in a joint test. These stresses are present in an actual truss, however. In addition, the effect of residual stresses in the welds on fatigue life may be more severe in a complete truss.

TABLE 4.1 Truss Test Results

Specimen	Stress Range (ksi)	Crack First Observed (cycles)	N Failure (cycles)
T1F	7.3	78,000	153,000
T2F	7.3	69,000	423,000
T3F	4.7	-	1,911,000
T4F	5.5	-	924,000

TABLE 4.2 Stresses in Truss Members

Member	Measured Stress (ksi)			Measured Average Stress (ksi)	Measured Force in Member (kips)	Calculated Force in Member (kips)
	T3F	T4F	T5F			
L0 L1	11.41	11.09	11.31	11.27	51.73	53.26
L1 L2	3.28	3.09	-	3.19	14.64	18.29
L2 U2	-3.81	-3.35	-3.77	-3.64	-29.41	-29.98
L1 U2	12.60	12.86	12.43	12.63	29.93	29.02
L1 U1	-11.57	-12.41	-12.76	-12.25	-29.03	-29.32
L0 U1	-11.51	-11.36	-11.66	-11.51	-93.00	-89.52
U1 U2	-7.99	-7.83	-	-7.91	-36.31	-35.72

TABLE 4.3 Stresses at K-Joint(Joint L1)

Strain Gauge Number	Measured Stress (ksi)	Calculated Stress (ksi)	Strain Gauge Number	Measured Stress (ksi)	Calculated Stress (ksi)
1	17.33	7.4	9	-27.57	-11.2
2	27.34	5.7	10	-15.78	-7.0
3	13.63	18.2	11	-3.66	-9.5
4	16.42	18.2	12	-5.51	-9.5
5	26.86	5.7	13	-16.66	-7.0
6	14.81	7.4	14	-29.97	-11.2
7	2.73	4.3	15	-16.93	-17.8
8	1.90	4.3	16	-16.81	-17.8

Note: Nominal Stress in Member L1 U1 = -11.6 ksi
U1 L2 = +12.6 ksi

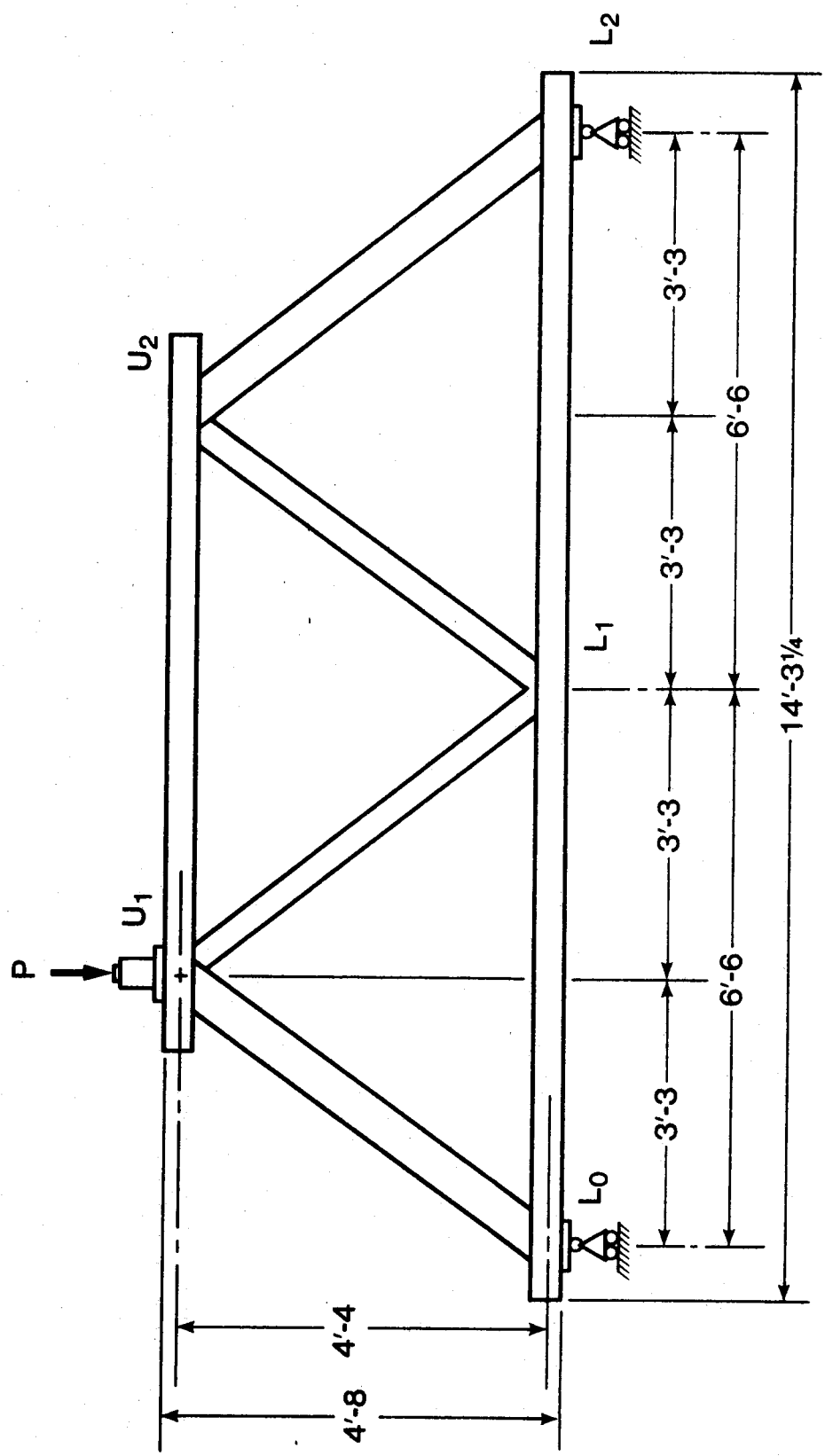

Figure 4.1 Truss specimen Layout

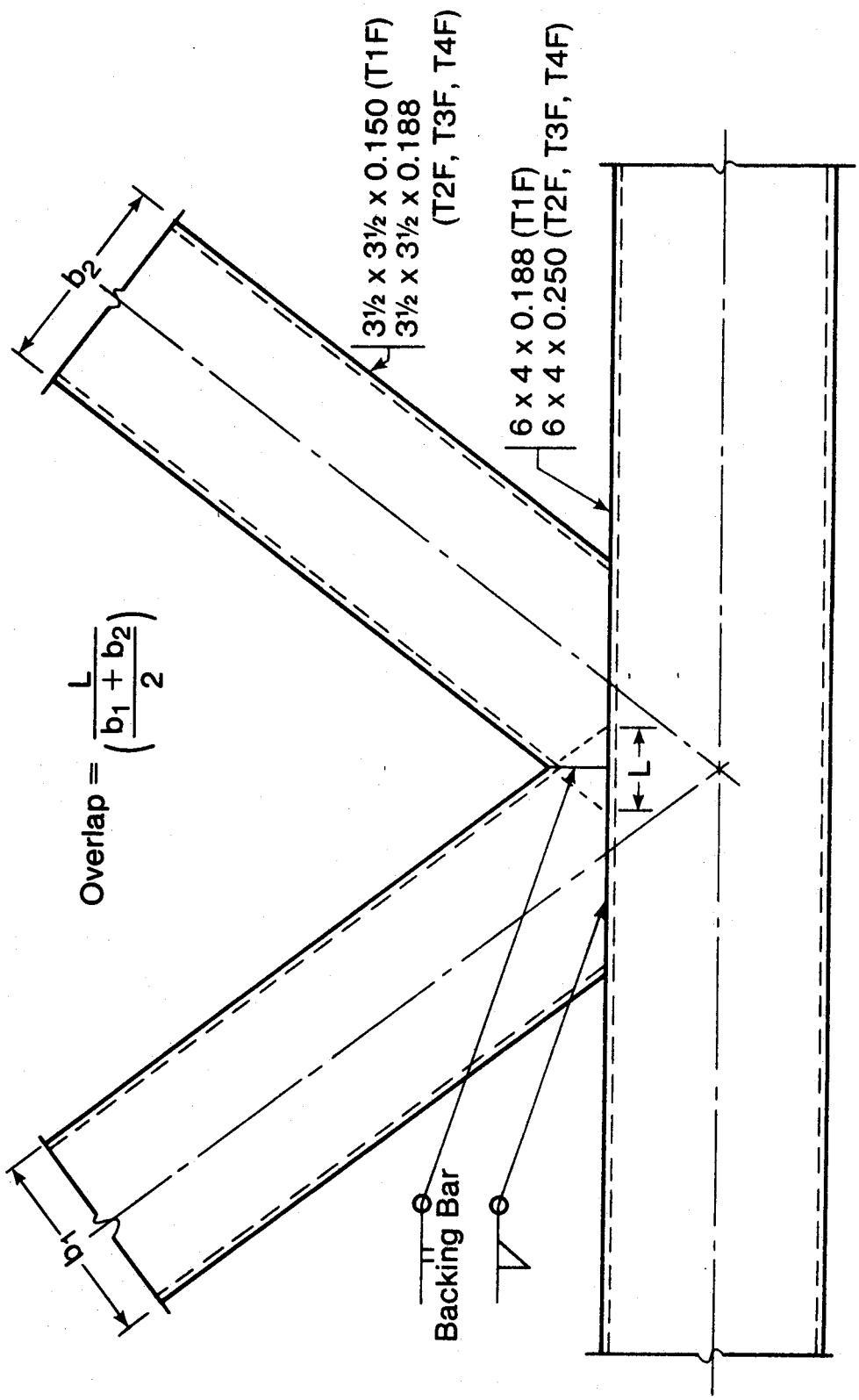

Figure 4.2 Details of Joint L1

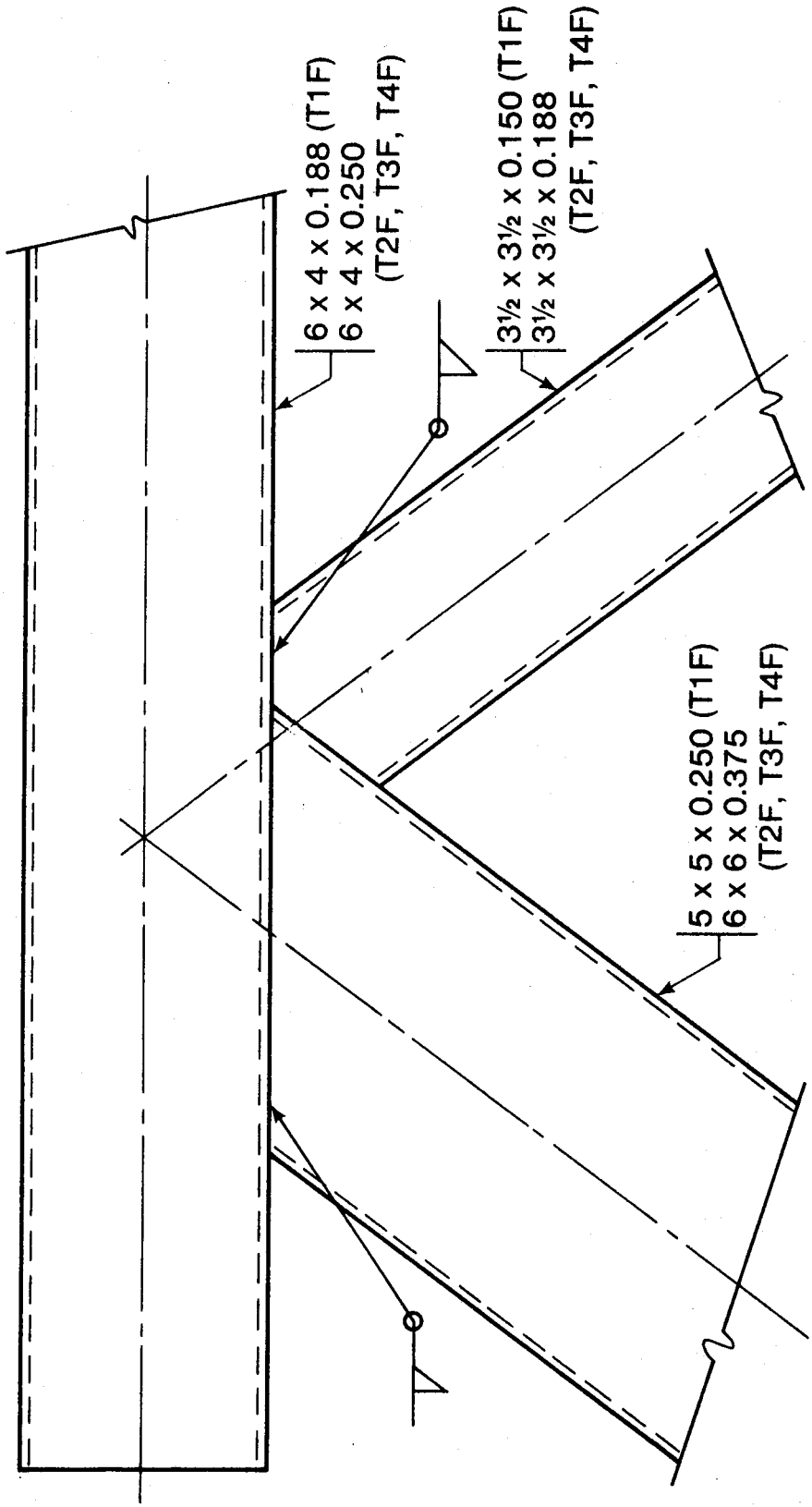

Figure 4.3 Details of Joints U1 and U2

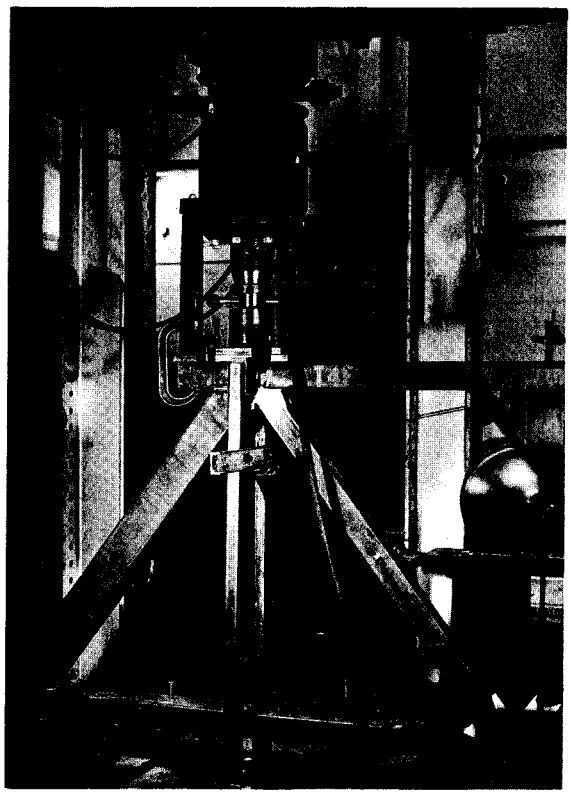

Figure 4.4 Test Set-Up

Figure 4.5 Crack at Joint L1

Figure 4.6 Crack at Joint L1 (opposite face)

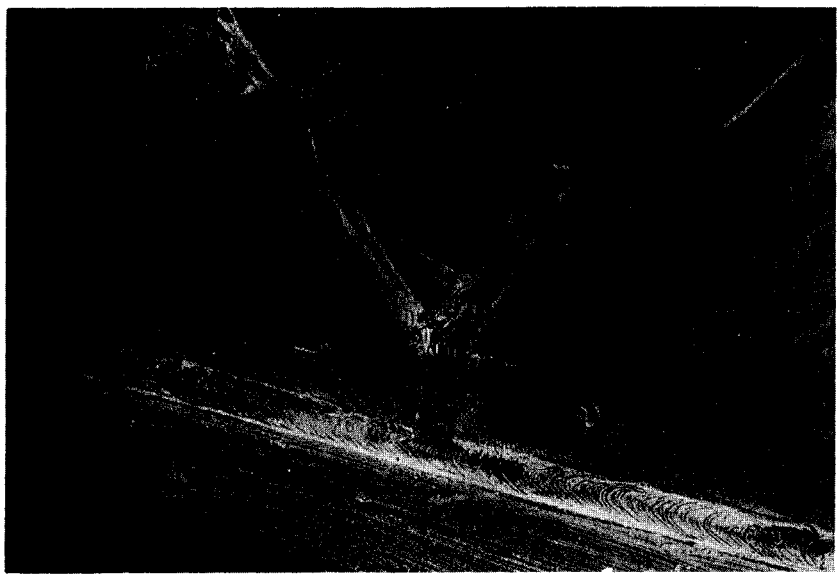

Figure 4.7 Crack at Joint L1 (T2F)

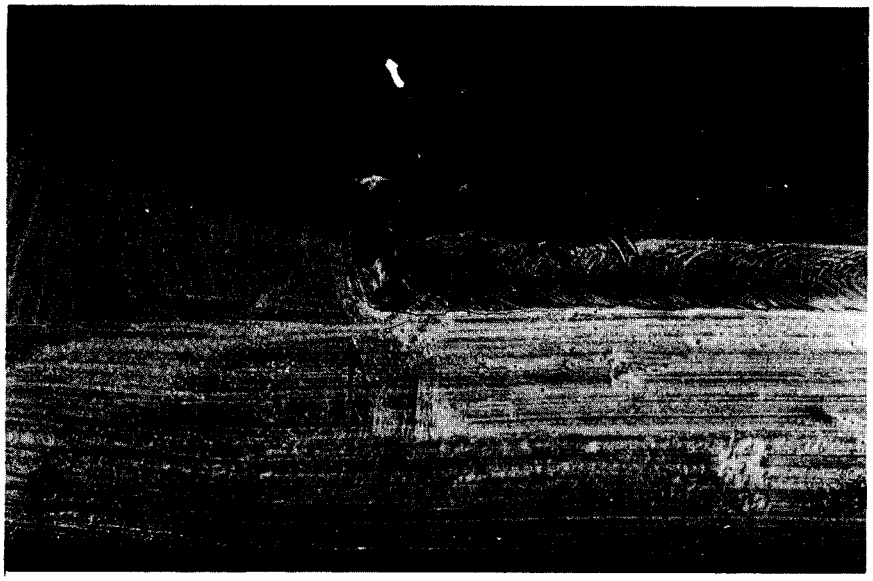

Figure 4.8 Crack at End of Member L1 U2

Figure 4.9 Crack at End of Member L1 U2 (joint U2)

Figure 4.10 Fracture Surface of Crack (joint U2)

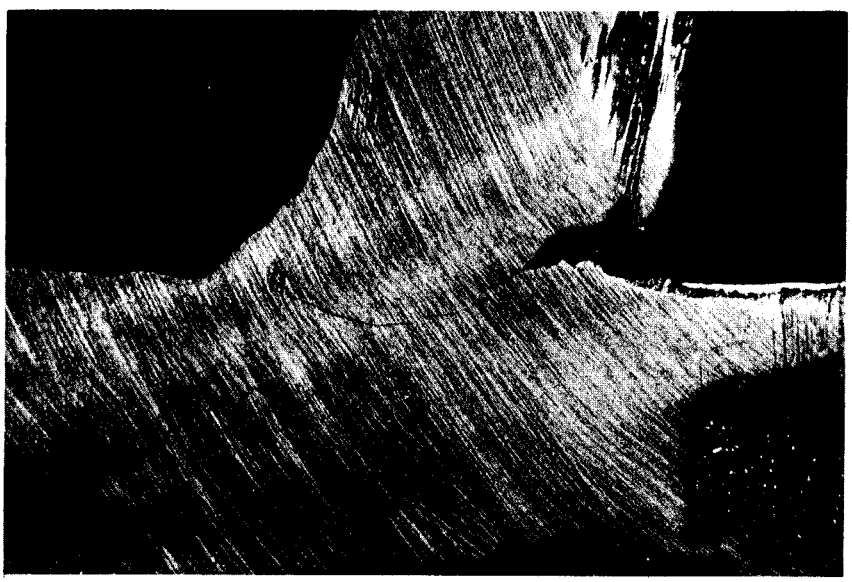

Figure 4.11 Crack Profile (joint U2)

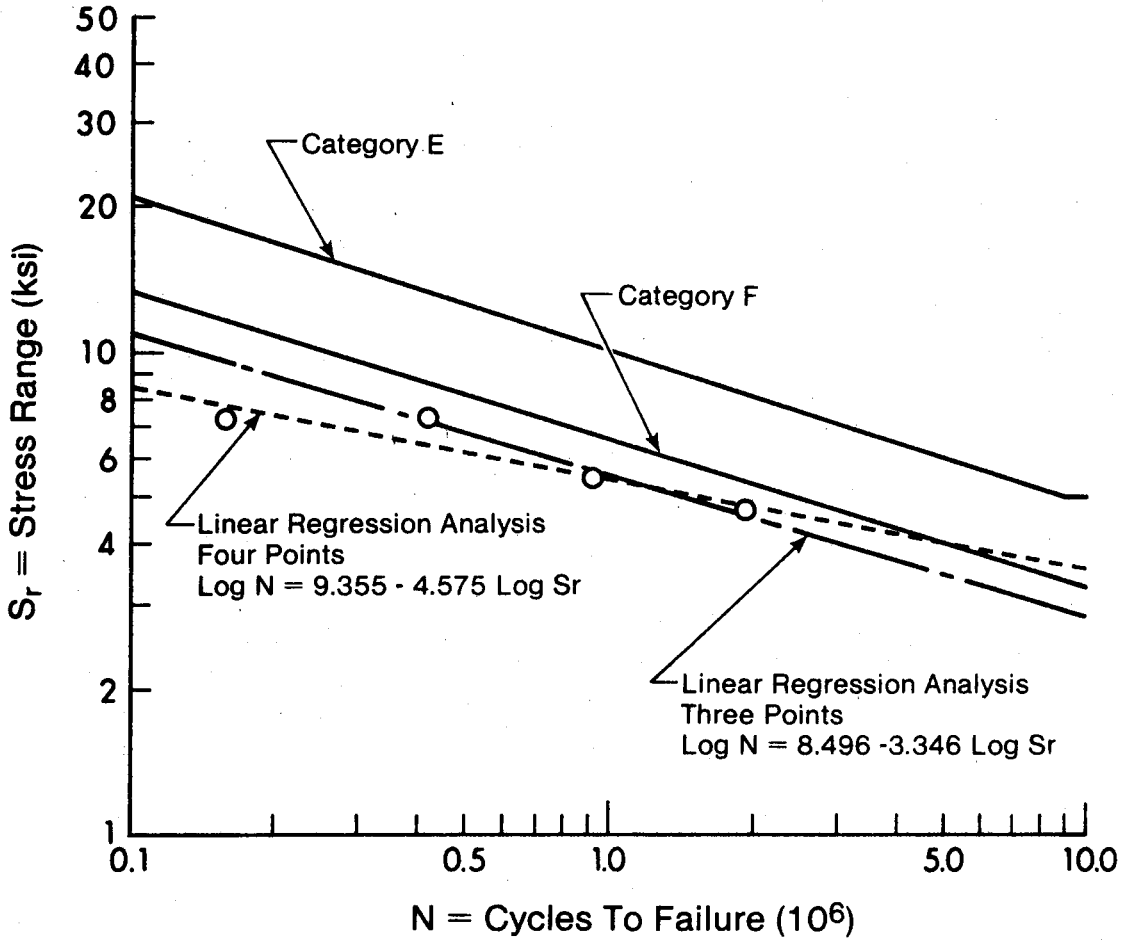

Figure 4.12 Hss Trusses With Welded Connections

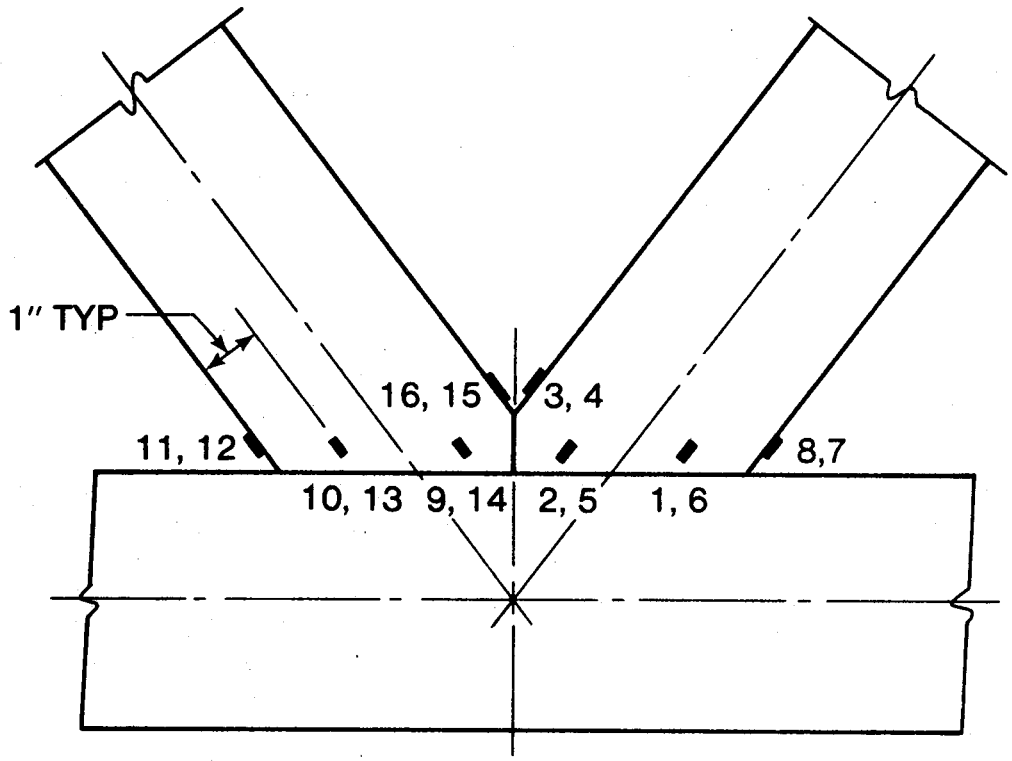

Note: Second number refers to gauge on opposite face with same relative location.

Figure 4.13 Strain Gauge Locations at K-Joint

5. SUMMARY AND CONCLUSIONS

5.1 Summary

In the first phase of this study, the fatigue behavior of fifteen beams with fillet welded attachments was investigated. Three beams with tapered transition lateral bracing attachments, and six beams with circular transition lateral bracing attachments were tested. One of the tapered transition attachments and all of the circular transition attachments had the toe of the fillet weld ground out. Also, six beams with plates welded to the webs were tested. These were tested to investigate the effect welding has on fatigue life when two members intersect at right angles. In addition to the experimental program, the results from the beams with plates welded to their webs were compared to a theoretical analysis based on a fracture mechanics approach.

The second phase of this study evaluated the fatigue life of four trusses made up of square and rectangular HSS sections with welded connections. The trusses had a center K-joint with a groove weld detail. All other joints were fillet welded. A discussion of the stress distribution in the truss members, and the stress distribution at the K-joint is presented.

In both phases of the study, the test results are compared to previous studies of welded details and to present design recommendations.

5.2 Conclusions

5.2.1 Beams With Tapered Transition Lateral Bracing Attachments

a. All beams in this series failed due to a vertical fatigue crack which initiated at the toe of the fillet weld or at a porosity in the fillet weld at the end of the bracing attachment. The crack then grew through the beam web.

b. Tapering the end of the lateral bracing attachment did not significantly improve the fatigue life of the detail as compared to providing a 90-degree change in direction.

c. These beams exhibited essentially the same fatigue behavior as a cover plated beam.

d. The fatigue strengths of beams in this series are satisfactorily described by CSA Category E.

5.2.2 Beams With Circular Transition Lateral Bracing Attachments

a. Except for one specimen which failed at the vertical stiffener, all beams in this series failed due to a vertical crack which initiated at a slag inclusion and/or porosity in the fillet weld near the end of the attachment. The crack then grew through the beam web.

b. None of the specimens tested failed at the location where the weld toe had been prior to grinding.

c. These beams exhibited fatigue lives significantly greater than cover plated beams.

5.2.3 Beams With Plates Intersecting the Webs

a. All beams in this series failed as a result of vertical fatigue cracks which initiated at the toe of the attachment fillet weld and grew through the beam web.
b. Details with plates passing through the beam web and details with plates interrupted at the beam web had essentially the same fatigue life.
c. The fatigue life is essentially the same as that of a cover plated beam.
d. The ratio of plate to web thickness did not influence the test results for the two values tested.

5.2.4 HSS Trusses With Welded Connections

a. Local stresses at a joint, in the vicinity of the welds, were up to 2.6 times greater than the nominal stress in the members coming into the joint.
b. In all cases, fatigue cracks causing failure initiated at the end of the diagonal in tension.
c. The fatigue lives observed in this test series were significantly lower than those permitted by current design recommendations.

5.3 Recommendations

The following recommendations are made relative to CSA Standard S16.1-1974, Supplement No. 1-1978, CSA Standard S6-1974, Supplement No.1-1976, and CSA Standard W59-1977.

a. Beams with tapered transition lateral bracing attachments could be designed as a Category E detail. However they provide no increase in fatigue life over a 90-degree change in direction.
b. Beams with fillet welded circular transition lateral bracing details and a 4 in. radius are properly classified as Category D.
c. Beams with members butting up against, or passing through their webs, and fillet welded, could be designed as a Category E detail. This should be permitted on the condition that inspection procedures are carried out to verify no lack of weld penetration exists in the joint.
d. A new fatigue category should be established for HSS trusses with welded connections. This category would predict lives which are less than those given by Category F.
e. Further tests should be done on beams with circular transition lateral bracing attachments to verify the further increase in fatigue life predicted by the CSA Standards for radii between 6 in. and 24 in., and radii greater than 24 in..
f. Further tests should be done on beams with lateral bracing attachments which are groove welded rather than fillet welded.
g. Further tests should be done on HSS trusses with welded joints using various lap geometries and member configurations. These tests should evaluate any difference in fatigue behavior which occurs between using groove welds and fillet welds.
h. Further tests should be carried out to establish a model for predicting the high local stresses which occur at welded HSS joints. These studies should also attempt to explain why the fatigue life of these joints is significantly lower than that of a cover plated beam.

REFERENCES

1. Rolfe, S.T., and Barsom, J.M., 'Fracture and Fatigue Control in Structures - Applications of Fracture Mechanics', Prentice-Hall Inc., New Jersey, 1977.
2. Gurney, T.R., 'Fatigue of Welded Structures', British Welding Research Association, London, 1968.
3. Fisher, J.W., Frank, K.H., Hirt, M.A., and McNamee,B.M., 'Effect of Weldments on the Fatigue Strength of Steel Beams', NCHRP Report 102, Transportation Research Board, Washington, 1970.
4. Fisher, J.W., Albrecht, P.A., Yen, B.T., Klingerman, D.J., and McNamee, B.M.,'Fatigue Strength of Steel Beams With Welded Stiffeners and Attachments', NCHRP Report 147, Transportation Research Board, Washington, 1974.
5. 'Design of Highway Bridges', CSA Standard S6-1974, Supplement No. 1-1976, Canadian Standards Association, Rexdale, Ontario.
6. 'Steel Structures For Buildings - Limit States Design', CSA Standard S16.1-1974, Supplement No. 1-1978, Canadian Standards Association, Rexdale, Ontario.
7. 'Welded Steel Construction (Metal-Arc Welding)', CSA Standard W59-1977, Canadian Standards Association, Rexdale, Ontario.
8. 'Standard Specification For Highway Bridges', American Association of State Highway and Transportation Officials, Washington, 1977.
9. Fisher, J.W., 'Classification of Welded Bridge Details For Fatigue Loading', NCHRP Research Results Digest 59, Highway Research Board, Washington, March 1974.
10. Gurney, T.R., 'Further Fatigue Tests on Mild Steel Specimens With Artificially Induced Residual Stresses', British Welding Journal, Vol. 9, No. 11, November 1962.
11. Bardell, G.R., and Kulak, G.L., 'Fatigue Behavior of Steel Beams With Welded Details', Structural Engineering Report No. 72, Dept. of Civil Engineering, University of Alberta, Edmonton, September 1978.
12. Babiker, D.B., 'The Fatigue Behavior of Welded Joints Between Structural Hollow Sections', University of Sheffield, Sheffield, England, 1967.
13. Eastwood, W., Osgerby, C., Wood, A.A., and Babiker, D.B., 'The Fatigue Behavior of Welded Joints Between Structural Hollow Sections', The University of Sheffield, Sheffield, England, July 1968.
14. Eastwood, W., Wood, A.A., and Opie, B.P., 'Further Fatigue Tests on the Fatigue Behavior of Welded Joints Between Structural Hollow Sections', The University of Sheffield, Sheffield, England, November 1970.
15. Eastwood, W., and Wood, A.A., 'Recent Research on Joints in Tubular Structures', Proceedings of the Canadian Structural Engineering Conference, February 1970, Canadian Steel Industries Construction Council, Toronto, Ontario, 1970.
16. Bouwkamp, J.C., and Stephen, R.M., 'Tubular Joints Under Alternating Loads (Phase II, Part 1)', University of California Structural Engineering Laboratory, November 1967.
17. Bouwkamp, J.C., and Stephen, R.M., 'Tubular Joints Under Alternating Loads (Phase II, Part 2)', University of California Structural Engineering Laboratory, March, 1970.
18. Tajima, J., Okukawa, A., Sugizaki, M., and Takenouchi, H., 'Fatigue Tests of a Panel Point Structures of Truss Made of 80 kg/mm2. High Strength Tensile Steel', IIW Document No. XII-831-77, July 1977.

19. Cran, J.A., Gibson, E.B., and Stadnyckyj, S., 'Hollow Structural Sections Design Manual For Connections', The Steel Company of Canada, Limited, Hamilton, Ontario, 1971.
20. Fisher, J.W., 'Bridge Fatigue Guide/ Design and Details', American Institute of Steel Construction, New York, N.Y., 1977.
21. 'Structural Quality Steels', CSA Standard G40.21-1973, Canadian Standards Association, Rexdale, Ontario.
22. Fisher, J.W., Haussamann, H., and Pense, A.W., 'Retrofitting Procedures for Fatigue Damaged Full Scale Welded Bridge Beams', Fritz Engineering Laboratory Report No. 417-3(79), Lehigh University, 1979.
23. Roberts, R., and Irwin, G., 'Fatigue and Fracture of Bridge Steels', Journal of the Structural Division, Proceedings of the ASCE, Vol. 102, No. ST2, February 1976.
24. Maddox, S.J., 'A Fracture Mechanics Analysis of the Fatigue Behavior of a Fillet Welded Joint', Welding Research International, Vol. 6, No. 5, 1976.
25. Paris, P., and Erdogan, F., 'A Critical Analysis of Crack Propagation Laws', Transactions of the ASME, Journal of Basic Engineering, Series D, 85, No. 3, 1963.
26. Irwin, G.R., 'Analysis of Stresses and Strains Near the End Of a Crack Transversing a Plate', Transactions of the ASME, Journal of Applied Mechanics, Vol. 24, 1957.
27. Gurney, T.R., 'Finite Element Analysis of Some Joints With the Welds Transverse to the Direction of Stress', Welding Research International, Vol. 6, No. 4, 1976.
28. Signes, E.G., Baker, R.G., Harrison, J.D., and Burdekin, F.M., 'Factors Affecting the Fatigue Strength of Welded High Strength Steels', British Welding Journal, Vol. 14, March 1967.
29. Watkinson, F., Bodger, P.H., and Harrison, J.D., 'The Fatigue Strength of Welded Joints in High Strength Steels and Methods For its Improvement', Proceedings of the Conference on Fatigue of Welded Structures, July 1970, The Welding Institute, Abington, Cambridge, England.
30. Barsom, J.M., 'Fatigue Crack Propagation in Steels of Various Yield Strengths', Transactions of the ASME, Journal of Engineering For Industry, Series B, 93, No. 4, November 1971.
31. Hirt, M.A., and Fisher, J.W., 'Fatigue Crack Growth in Welded Beams', Engineering Fracture Mechanics, Vol. 5, No. 2, June 1973.
32. Slockblower, R.E., and Fisher, J.W., 'Fatigue Resistance of Full Scale Cover Plated Beams', Fritz Engineering Laboratory Report No. 386-9(78), Lehigh University, June 1978.
33. Maddox, S.J., 'An Analysis of Fatigue Cracks in Fillet Welded Joints', International Journal of Fracture, Vol. 11, No. 2, April 1975.
34. Maddox, S.J., 'Calculating the Fatigue Strength of a Welded Joint Using Fracture Mechanics', Metal Construction and British Welding Journal, Vol. 2, August 1970.
35. Albrecht, P., and Yamada, K., 'Rapid Calculation of Stress Intensity Factors'. Journal of the Structural Division, Proceedings of the ASCE, Vol. 103, No. ST2, February 1977.
36. Zettlemoyer, N., and Fisher, J.W., 'Stress Gradient Correction Factor For Stress Intensity at Welded Stiffeners and Cover Plates', Welding Journal, Vol. 56, No. 12(Supplement), December 1977.
37. Kreysig, E., 'Introductory Mathematical Statistics', John Wiley and Sons, Inc., New York, N.Y., 1970.